Pergamon

Geochimica et Cosmochimica Acta, Vol. 67, No. 12, pp. 2117–2136, 2003

0016-7037/03 $30.00 + .00

doi:10.1016/S0016-7037(02)01306-6

The groundwater geochemistry of the Bengal Basin: Weathering, chemsorption, and trace metal flux to the oceans

CAROLYN B. DOWLING,* ROBERT J. POREDA, and ASISH R. BASU
Department of Earth and Environmental Sciences, University of Rochester, Rochester, NY 14627, USA

(*Received June* 19, 2002; *accepted in revised form September* 18, 2002)

Abstract—Sixty-eight groundwater samples from the Ganges-Brahmaputra floodplain in the Bengal Basin were analyzed to assess the groundwater geochemistry, the subsurface hydrology, the buffering effects of sediments on trace metal concentrations and their isotopic compositions, and the magnitude of the subsurface trace element flux to the Bay of Bengal and to the global ocean. Samples obtained from depths of 10 to 350 m were measured for major and trace elements, dissolved gas, and tritium. On the basis of the $^{3}He/^{3}H$ ages, the groundwater at depth (30–150 m) appears to be continually replenished, indicating that this recharge of groundwater to depth must ultimately be balanced by a significant quantity of submarine discharge into the Bay of Bengal. Using the $^{3}He/^{3}H$ groundwater age–depth relationship to calculate a recharge rate of 60 ± 20 cm/yr, we estimate a subsurface discharge into the Bay of Bengal of $1.5 \pm 0.5 \times 10^{11}$ m^3/yr, or 15% of the surface Ganges-Brahmaputra river (GBR) flux. Several trace elements, especially Sr and Ba, display elevated concentrations averaging 7 to 9 times the surface GBR water values. The submarine groundwater fluxes of Sr and Ba to the oceans are $8.2 \pm 2 \times 10^{8}$ and $1.5 \pm 0.3 \times 10^{8}$ mol/yr, or 3.3 and 1.2%, respectively, of the world total, or equal to the surface GBR Sr and Ba estimated fluxes. Our groundwater flux for Ba agrees with the estimate of Moore (1997) (3×10^{8}–3×10^{9} mol/yr), on the basis of measured Ba and Ra excesses in the Bay of Bengal. Other trace metals, such as U and Mo, are at low but measurable levels and are not major contributors to the global flux in this river system. A comparison of the Sr and Ba concentrations, plus $^{87}Sr/^{86}Sr$ ratios in groundwater to the oxalate extractable fractions of a coastal sediment core, suggests that weathering of carbonates and minor silicates, coupled with cation exchange plus adsorption and desorption reactions, controls the trace element concentrations and $^{87}Sr/^{86}Sr$ isotopic compositions in both the groundwater and river water. Our data also imply that other coastal floodplains (e.g., the Mekong and the Irrawaddy rivers) that have high precipitation rates and rapid accumulation of immature sediments are likely to make significant contributions to the global oceanic trace metal budgets and have an impact on the Sr isotopic evolution in seawater. *Copyright © 2003 Elsevier Science Ltd*

1. INTRODUCTION

Chemical weathering resulting from the uplift and erosion of mountain belts strongly influences the dissolved trace metal flux to the oceans via rivers and groundwater discharge. The riverine and groundwater fluxes into the oceans are important for geochemical and climate models as well as for calculating elemental and isotopic budgets and residence times of elements in the ocean (e.g., the increase in oceanic $^{87}Sr/^{86}Sr$ in the Cenozoic). When estimating the flux of trace elements and nutrients to the coastal oceans, most studies consider only the surface discharge of the major rivers (e.g., Palmer and Edmond, 1989). Trace metal flux through groundwater discharge often has been neglected or overlooked because it represents a non-point source, occurs over a broader subterranean area, and thus is more difficult to quantify. However, several recent studies have shown that the influence of groundwater discharge can be substantial because of higher concentrations of certain trace metals and nutrients from the infiltration of fertilizers, the weathering of the aquifer protoliths, and redox controls of adsorption and desorption reactions (Loeb and Goldman, 1979; Johannes, 1980; Bokuniewicz and Pavlik, 1990; Burnett et al., 1990; Giblin and Gaines, 1990; LaPointe et al., 1990; Oberdorfer et al., 1990; Valiela et al., 1990, 1992; Moore, 1996, 1997). Unaccounted groundwater fluxes will have a significant impact on continental erosion rate estimates, global geochemical models, and climate models based on carbon dioxide consumption via weathering reactions.

In an effort to understand the magnitude of the groundwater discharge and the trace metal fluxes to the coastal oceans, we examined the surface and groundwater chemistry of one of the world's largest river systems, the Ganges-Brahmaputra river (GBR). The GBR drains the rapidly weathering, tectonically active Himalayan mountain range and carries the single largest sediment flux and the fourth highest water discharge to the oceans (Holeman, 1968; Coleman, 1969; Milliman and Meade, 1983). The GBR flows to the Bay of Bengal, where its sediment load is deposited to form the deep-sea Bengal fan. The GBR is often cited as influencing ocean chemistry through its unique river water and large flux of immature sediment from the weathering of the Himalayas (Raymo et al., 1988; Palmer and Edmond, 1989; Richter et al., 1992; Godderis and Francois, 1995; Harris, 1995; Derry and France-Lanord, 1996; Chesley et al., 2000). The flux and isotopic ratio of strontium from the GBR to the ocean has become a matter of controversy in terms of its lithologic source (silicate vs. carbonate) and its corresponding isotopic ratio (Edmond, 1992; Krishnaswami et al., 1992; Palmer and Edmond, 1992; Derry and France-Lanord,

* Author to whom correspondence should be addressed, at Byrd Polar Research Center, The Ohio State University, Scott Hall, 1090 Carmack Road, Columbus, OH 43210-1002, USA (dowling.37@osu.edu).

1996; Quade et al., 1997; Blum et al., 1998; Singh et al., 1998; Galy et al., 1999; English et al., 2000).

Most of the investigations concerning the water chemistry of the GBR have focused on the influence of the mountainous headwater regions on the observed downstream river chemistry. Few large-scale studies have focused exclusively on the GBR floodplain and its subsurface hydrology. The deltaic groundwater may have a major impact on river and oceanic chemistry (e.g., trace metal fluxes and the $^{87}Sr/^{86}Sr$ marine record) through the weathering of aquifer protolith, adsorption and desorption reactions, and groundwater discharge to the Bay of Bengal and the GBR. The purpose of this study is to characterize the hydrogeology of the Bengal Basin, examine the impact that floodplain sediments have on the strontium isotopic composition of the groundwater and river water, and determine the subsurface discharge of trace metals into the coastal ocean from the GBR floodplain. To quantify groundwater travel times and groundwater flow in Bengal Basin, we used tritium, ^{3}He, and ^{4}He concentrations. We estimated the groundwater fluxes by determining the $^{3}He/^{3}H$ ages of the groundwater and then combining the results with our dissolved groundwater trace metal concentration data. Sediment extraction experiments were performed to determine the role of cation exchange and adsorption and desorption reactions on sedimentary grain surfaces in controlling the trace metal concentrations and their isotopic compositions in the ground and surface waters. Given the constraints on the flux and Sr concentrations given in this study and using the same samples, Basu et al. (2001) showed that the $^{87}Sr/^{86}Sr$ ratio of the ocean can be strongly influenced by submarine discharge from the Bengal Basin.

2. GEOLOGY OF THE GANGES-BRAHMAPUPTRA FLOODPLAIN

The drainage area of the GBR is $\sim 2 \times 10^6$ km^2 (Holeman, 1968; Coleman, 1969), and its floodplain in Bangladesh and India is estimated to be 2.5×10^5 km^2 (modified from Morgan and McIntire, 1959). The discharge of the GBR to the Bay of Bengal varies considerably over the year; Subramanian (1979) reported a total yearly discharge of $1.0 \pm 0.1 \times 10^{12}$ m^3. The Ganges River flows through highly weathered sediments, resulting in a heavy clay load, whereas the Brahmaputra River drains very young and unweathered sedimentary rocks, producing a silty and sandy bedload (Coleman, 1969). Galy et al. (1999) and Galy and France-Lanord (2001) reported that the GBR sediment load is composed of quartz, clays, primary micas, and carbonates. Coleman (1969) pointed out that despite the large sediment load to the Bay of Bengal (ranked first in the world on the basis of mass), the shoreline is relatively stable, with sediment deposition balancing subsidence. Most of the sediment is channeled into deeper water through a deep submarine canyon, the Swatch of No Land, creating one of the largest global submarine deltas, the Bengal fan.

Within the GBR floodplain, the Bengal Basin consists of mostly quaternary deltaic sediments of the GBR and the alluvial deposits from the weathering of the Himalayas. In the basin, the nature of sediment deposition has been sensitive to the relative rates of sea level rise and sediment input from the rivers throughout geologic time. During high sediment input, rapid aggradation of fluvial channel sediment and progradation of lobate deltas occur. Conversely, when sea level is high, relatively large estuaries receive dominantly fine-grained sediments. The hydrology of the Bengal Basin is complex because of the complicated interfingerings of coarse and fine-grained sediments from the numerous regressions and transgressions. Silts and sands dominate the upper valley deposits, whereas in the lower delta, there are silts, clays, and peats (Coleman, 1969). The floodplain soils in the delta are a mixture of clays, quartz, calcium carbonate, dolomite, and mica (Food and Agriculture Organization, 1971). The British Geological Survey (1999) summarized the quaternary stratigraphy of the lower floodplain (Bangladesh), and Uddin and Lundberg (1998) resolved four subsurface stratigraphy columns to the Precambrian in Bangladesh. The mineralogy of the aquifers is important because the weathering of the protolith has a major impact on groundwater chemistry. In general, the subsurface mineralogy of the Ganges-Brahmaputra delta is dominated by quartz (ranging from 57–99%), with some plagioclase and potassium feldspar (ranging from 0–23%) and volcanic, metamorphic, and sedimentary fragments (ranging from 0–20%) (Uddin and Lundberg, 1998). Coal, limestone, and mica (mostly biotite) are found at depth (Uddin and Lundberg, 1998).

3. SAMPLING AND METHODOLOGY

In May 1999 and January 2000, we sampled a total of 68 groundwater samples from monitoring and domestic wells in the Ganges-Brahmaputra delta throughout Bangladesh and parts of West Bengal, India, according to standard methods (Fig. 1) (Long and Martin, 1991; Greenberg et al., 1992). The sediment drill core was taken adjacent to the multilevel well cluster at Laxmipur (Fig. 1). W. S. Moore (University of South Carolina) provided the river sediment samples upstream from the confluence of the Ganges (RW-54) and Brahmaputra (RW-53) rivers (Sarin et al., 1989), and A. R. Basu collected samples on the northern GBR.

Field parameters, pH, temperature, conductivity, bicarbonate, and latitude and longitude (using the Global Positioning System) were recorded at each well site. Groundwater samples for major element (cations and anions) and trace metal analyses were collected through 0.25-μm polycarbonate filters at the field collection sites. For the trace metal and cation samples, the filtered water was acidified to $\sim$pH 2 with ultrapure nitric acid on site. The samples for dissolved gas content and helium isotope analysis were collected using 0.375-inch (inside diameter) copper tubes and sealed with refrigeration clamps according to methods established in and used since the early 1970s (e.g., Poreda et al., 1988). Water samples for tritium analysis were stored in amber glass bottles with polyethylene caps to minimize water-vapor exchange.

Major cations and anions in the groundwater samples were measured on a Dionex ion chromatograph (IC) according to our established procedures at the University of Rochester (e.g., Fehn et al., 2000). We used CS12A and AS4A Ion Pac columns to analyze the cations and anions, respectively. Cation and anion aqueous standards were used to calibrate the IC after every two water samples that were analyzed. The analytical errors for these IC analyses were usually $< 6\%$ for the cations

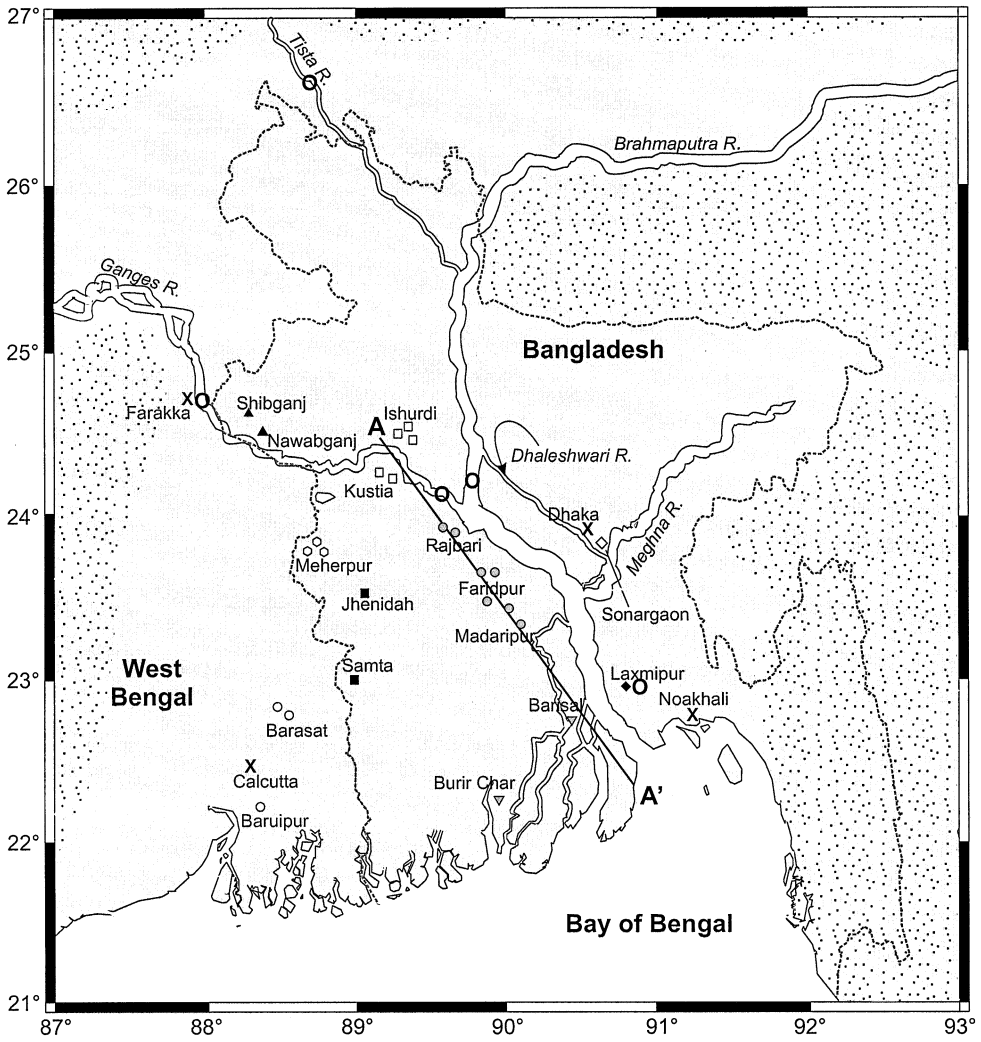

Fig. 1. Bengal Basin groundwater and river sediment collection sites. This map of the Bengal Basin shows the location of groundwater (variety of symbols) and river sediment (O) samples in Bangladesh and India. The sediment samples (O) are from Laxmipur and the Ganges and Brahmaputra rivers (collected by W. S. Moore). The letter X designates the larger towns. The floodplain is designated by the solid gray color; the stippled areas are not included in our floodplain area estimate.

and anions. Gas concentrations and isotopic ratio measurements of the groundwater samples were carried out at the Rare Gas Facility at the University of Rochester. The dissolved gas was extracted and processed on a high vacuum line (Poreda et al., 1988). The dissolved gas samples were hermetic because there was no measurable oxygen in the samples. Although we cannot rule out some gas loss in those samples that contained $pCH_4 > 2$ atm (e.g., BGD 3–8 and BGD 30–35), the clamps have proved effective in sampling waters that contain < 10 atm of CH_4 (e.g., Lakekiru). The helium isotope ratio measurements were made with a VG 5400 noble gas mass spectrometer by peak height comparison to a calibrated air standard, with errors of ~2% (Poreda and Farley, 1992). Helium isotope ratios are expressed as R/R_{air}, where R is the $^3He/^4He$ ratio in the sample and R_{air} is the $^3He/^4He$ ratio in the air standard. Errors in the reported values of R/R_{air} are ~0.5%. The tritium values were determined using the ^3He "in-growth" technique (Clarke et al., 1976). The errors depend on the amount of ^3H and are ±5% at 10 tritium units (TU).

Tritium (^3H) is a radioactive isotope of hydrogen with a half-life of 12.43 yr and is a useful tracer in post–nuclear age groundwater. Tritium activity in atmospheric precipitation before 1953 has been estimated to be < 20 TU at high latitudes and may have been < 5 TU (Kaufman and Libby, 1954; Robertson and Cherry, 1989). During the height of nuclear bomb testing (the mid-1960s), the tritium in atmospheric precipitation increased dramatically to > 3000 TU in the interior regions of the Northern Hemisphere. However, much lower levels occurred in the coastal and low-latitude regions such as Bangladesh, especially where the dominant source of moisture is from the monsoons. Tritiogenic helium ($^3He^*$) is the stable decay product of tritium and can be used in combination with tritium levels to date groundwater (e.g., Poreda et al., 1988; Schlosser, 1992; Solomon et al., 1992, 1995). Once the water

enters into the water table and becomes isolated from the atmosphere, tritiogenic ^{3}He* is directly derived from the decay of tritium. The ^{3}He/^{3}H age then is defined as $t(^3\text{He}/^3\text{H}) = \lambda^{-1}\ln[(^3\text{He}^*/^3\text{H}) + 1]$.

Total concentration and isotopic composition of helium and neon for the drill core quartz separates were determined by fusing ~100 to 200 mg of sample at 1800°C in a modified Turner double-walled furnace and measured on a VG 5400 noble gas mass spectrometer (Poreda and Farley, 1992). An air standard of known volume was used to calibrate He and Ne. The mineralogical composition of the Laxmipur sediment core was determined by X-ray diffraction (XRD) analysis using a Scintag XDS 2000 instrument. The clay-sized particles were separated using floatation, and the micas were separated from the bulk sediment by hand using a Nikon SMZ-U microscope. For the bulk and fine-grained sediments and mica separates, the exchangeable and adsorbed trace metals were extracted using an ammonium oxalate acid reagent (McKeague, 1978). Ten milliliters of 0.2-mol/L oxalate solution were added to 0.25 g of sediment (or any proportion thereof) and agitated horizontally for 4 h in the dark. The clay-sized particles and micas were then rinsed with 18 MΩ water, dried, and digested using a Milestone MLS 1200 microwave digestion system. The digested samples were evaporated to dryness and reacidified using ultrapure nitric acid.

Iron concentrations for groundwater and sediment extracts were determined using a Shimandzu ultraviolet (UV)–visible spectrophotometer. We prepared the samples by adding hydroxylamine hydrochloride (10% w/v), FerroZine iron reagent, and ammonium acetate buffer solution (ammonium hydroxide and ultrapure glacial acetic acid) to them (To et al., 1999). Errors in the UV-visible calibration curves were generally < 3%. To prepare the groundwater, sediment extracts, and sediment digestions for trace metal analysis by inductively coupled plasma mass spectrometry (ICP-MS), the samples were further diluted with 18 MΩ water and again acidified with ultrapure nitric acid. The analyses were done on the VG ICP-MS Plasma Quad II+ at the University of Rochester according to U.S. Environmental Protection Agency method 200.8 (Long and Martin, 1991). To correct for drift, gallium, indium, and bismuth were added as internal standards for the water and oxalate extraction samples. For the sediment digestions, only indium and bismuth were used. A five-point calibration curve was created using 0.1-, 1-, 10-, 30-, and 75-ppb standards. The standards, traceable to the National Institute of Standards and Technology (NIST), were analyzed before and after a set of samples. Two NIST water standards (NIST 1640 and NIST 1643d) were analyzed as unknowns. On the basis of these results, the errors in the trace metal concentration analyses were < 5% for the samples measured with the VG ICP-MS Plasma Quad II+. The strontium isotopes (^{87}Sr/^{86}Sr) of the groundwater and sediment extraction samples were measured by thermal ionization mass spectrometry at the University of Rochester (Basu et al., 1999). The measurements were normalized to ^{86}Sr/^{88}Sr (0.1194), and the National Bureau of Standards 987 Sr standard gave a strontium isotopic measurement of 0.710246 ± 28 during the course of the measurements. Errors in the Sr isotope ratio measurements are better than 4 in the fifth decimal place (0.00004), corresponding to the 2σ of the mean.

4. RESULTS

4. Groundwater Ages

Table 1 lists the dissolved gas concentrations (He, Ne, N_2, Ar, and CH_4), helium isotopes, tritium, and calculated ^{3}He/^{3}H ages for each groundwater sample. Using the presence of tritium to indicate nuclear age water (post-1950), we note that 25% of the wells, including several municipal wells, contain tritium (0.2–8.4 TU). In some areas, the tritiated water is found to a depth of 150 m, indicating highly conductive sediments. In contrast, the groundwater from the piezometer clusters at Laxmipur (BGD 31–35) and Faridpur (BGD 3–8) contains tritium only in the shallowest 10- and 20-m samples. The samples below 20 m are tritium free (<0.15 TU), a characteristic of low-permeability sediments and groundwater residence times of > 50 yr. Fine-grained sediments of low permeability, such as silts and clays, dominate the depositional environment in the Laxmipur and Faridpur regions.

For samples that contain tritium, the ratio of tritiogenic helium (^{3}He*) to ^{3}H gives an approximate subsurface travel time or "groundwater age." In Figure 2, the ^{3}He/^{3}H groundwater ages are plotted against depth to examine the contrast in vertical groundwater velocities (Solomon et al., 1993, 1995). The velocity ranges from 3 m/yr in the active flow system to <0.5 m/yr in the low-conductivity sediments of Laxmipur and Faridpur. This extreme contrast in vertical velocities suggests that complex interfingerings of high- and low-conductivity layers exist within the subsurface, which is consistent with the floodplain setting. Figure 2 establishes the range of groundwater recharge rates to be 10 to 100 cm/yr, with an average of 60 ± 20 cm/yr. In these highly conductive sediments, rainwater is quickly recharged to depth and rapidly flushed through the sediments over a wide area in the GBR floodplain. Our groundwater recharge values are calculated by dividing the depth (z) below the water table by the ^{3}He/^{3}H groundwater age and then multiplying by the porosity ($z \times \Theta$/age). Thus, the groundwater table fluctuations and year-to-year seasonal variations are averaged out. The groundwater ages measure the residence time of the groundwater in the aquifers and do not differentiate between wet and dry season recharge. This rapidly recharged water as well as the groundwater flowing well beneath the river bottom (>30 m) does not discharge to the GBR or its tributaries. Because of the low horizontal hydraulic gradient ($>10^{-4}$) and high vertical gradients, a regional flow net (not shown) has groundwater moving deeper into the system until it encounters the seawater-freshwater interface. Hydraulic heads decrease with depth (i.e., vertical gradients are always down), except in the deepest artesian wells (>250 m). On the basis of an average vertical velocity of 2 m/yr and the average recharge rate of 60 ± 20 cm/yr, an enormous amount of water is rapidly flowing into the aquifers below 30 m that ultimately must be balanced by discharge to the coastal ocean.

Alternatively, the groundwater age gradient that we observe could also be from groundwater withdrawal for agriculture; however, by our calculations, the groundwater resources of the Bengal Basin are underutilized. On the basis of a British Geological Survey (1999) report, $\sim 2.1 \times 10^{10}$ m^3/yr of groundwater, or 12 ± 4% of our recharge estimate, is withdrawn for agricultural and domestic use in the Bengal Basin.

Table 1. Dissolved gas data and ages of the Bengal Basin groundwaters. The sample locations are shown in Fig. 1.

Sample name	Sample location	Depth (m)	Total ^{4}He (μc/kg)	Radiogenic ^{4}He (μc/kg)	Ne (μc/kg)	N_2 (c/kg)	Ar (c/kg)	CH_4 (c/kg)	R/R_{air}[a]	^{3}H[b] (TU)	age (yr) ^{3}He/^{3}H
BGD 2	Sonapur	11	c	c	c	c	c	c	c	2.4	<20
BGD 3	Faridpur	20	18.6	9.1	62.2	5.4	0.2	23.6	0.90	<0.15	>80
BGD 4	Faridpur	30	18.9	0.0	77.1	5.8	0.2	20.6	0.94	<0.15	>80
BGD 5	Faridpur	40	25.1	3.6	103.2	6.6	0.2	11.9	0.92	<0.15	>80
BGD 6	Faridpur	150	99.1	72.9	106.5	8.1	0.2	0.3	0.53	<0.15	>80
BGD 7	Faridpur	50	36.9	2.9	140.8	8.9	0.2	6.8	0.96	<0.15	>80
BGD 8	Faridpur	244	53.2	29.9	109.8	7.6	0.2	28.4	0.55	<0.15	>80
BGD 9	Faridpur	98	53.6	28.9	119.4	7.6	0.2	0.2	0.56	<0.15	>80
BGD 10	Ahladipur	30	39.4	–1.9	171.0	16.1	0.3	0.2	2.51	8.4	28.5
BGD 11	Rajbari	48	c	c	c	c	c	c	c	4.2	<20
BGD 12	Rajbari	33	c	c	c	c	c	c	c	6.2	30
BGD 13	Rajbari	127	66.2	–1.0	260.9	14.6	0.339	0.2	1.03	0.5	50
BGD 14	Talma	44	55.9	28.7	101.0	5.8	0.163	16.4	0.49	c	c
BGD 15	Nagarkanda	29	52.1	5.0	184.2	10.9	0.264	6.0	0.85	0.3	>80
BGD 16	Samta	9	26.5	3.2	109.6	9.7	0.198	3.9	1.84	8.4	17.9
BGD 17	Samta	49	44.6	–5.6	191.4	11.2	0.251	6.6	1.03	0.2	40.1
BGD 18	Samta	61	c	c	c	c	c	c	c	<0.15	>80
BGD 20	Jhenidah	100	65.6	–6.5	271.9	14.5	0.313	0.1	1.78	5.8	30.3
BGD 21	Burir Char	61	51.7	–2.7	210.8	11.5	0.284	0.2	2.39	4.8	40.0
BGD 22	Burir Char	152	c	c	c	c	c	c	c	<0.15	c
BGD 23	Burir Char	280	5302.1	5276.0	116.8	10.7	0.280	173.2	0.09	<0.15	>100
BGD 24	Barishal	335	3277.8	3109.4	610.7	36.7	0.641	12.4	0.30	<0.15	>100
BGD 25	Barishal	290	895.2	845.1	200.0	14.6	0.213	3.6	0.29	<0.15	>100
BGD 26	Madaripur	30	53.8	–5.1	233.1	14.0	0.330	0.6	1.05	3.4	8.4
BGD 27	Choto Arjundi	27	40.1	–6.7	169.2	8.9	0.194	4.6	1.17	0.8	36.6
BGD 28	Mugraoara	c	c	c	c	c	c	c	c	<0.15	c
BGD 29	Patalpara	c	51.0	12.4	144.1	9.0	0.201	14.5	0.76	0.3	50
BGD 30	Adampur	91	311.5	265.8	184.9	11.6	0.294	0.0	0.45	<0.15	>80
BGD 31	Laxmipur	50	3.5	8.6[d]	8.6	1.1	0.041	34.7	0.76	0.4	>80
BGD 32	Laxmipur	40	3.9	8.9[d]	8.9	1.4	0.051	46.1	0.66	0.2	>80
BGD 33	Laxmipur	30	3.8	8.9[d]	8.4	1.5	0.061	42.6	0.73	<0.15	>80
BGD 34	Laxmipur	20	8.8	1.3	23.0	2.4	0.083	38.9	0.79	0.2	>80
BGD 35	Laxmipur	10	c	c	c	c	c	c	c	2.8	<20
BGD 36	Laxmipur	150	73.2	26.3	180.6	9.8	0.248	0.1	0.59	0.4	51.9
BGD 40	Nawabganj	34	c	c	c	c	c	c	c	<0.15	c
BGD 44	Baghail Dotala Sako	35	67.3	1.5	260.7	16.4	0.365	0.1	1.45	5.3	27.1
BGD 48	Refugee Para	27	53.2	–4.5	223.8	14.1	0.299	0.1	1.32	2.7	23.9
BGD 53	Kustia	37	82.0	25.6	231.8	18.5	0.374	4.3	1.00	<0.15	>80
IND 1	Moyna	50	57.5	–1.9	228.2	13.5	0.293	1.5	1.41	3.3	28.5
IND 3	Moyna	47.2	60.3	2.0	227.0	14.0	0.306	0.0	1.18	0.6	46.3
IND 4	Moyna	18.3	78.3	–4.1	297.4	15.1	0.278	12.7	1.15	1.8	23.0
IND 6	Birohi	18.3	40.4	–2.2	167.2	10.4	0.248	5.0	1.85	3.7	32.1
IND 9	Baruipur	293	254.6	188.5	261.4	15.4	0.363	0.2	0.37	<0.15	>100

[a] R is the ^{3}He/^{4}He in the sample, and R_{air} is the ^{3}He/^{4}He in the air standard.
[b] ^{3}H is measured in tritium units (TU).
[c] Data not available.
[d] See explanation in text.

Pumping will have a significant effect on the groundwater resources only if the withdrawal had taken place at 6 to 10 times the current level for the past 30 yr.

Figure 3 is a schematic cross-section of the groundwater flow in the Bangladesh part of the Bengal Basin from NW to SE (A-A' in Fig. 1). The figure divides wells into several groups on the basis of the dissolved ^{4}He, ^{3}H, and ^{3}He/^{3}H age data. In the upper aquifer (<100 m), there are municipal wells that contain tritium with ^{4}He, N_2, and Ar at their solubility levels. Shallow wells (<60 m) at Laxmipur, Faridpur, and Kustia are tritium dead and have low dissolved atmospheric gas but high biogenic CH_4 concentrations. Laxmipur and Faridpur water samples have suffered variable amounts of gas loss because of elevated levels of dissolved biogenic methane in these waters. Three wells (BGD 31–33) in Laxmipur are stripped of the majority of their dissolved gases, including helium, neon, nitrogen, and argon. However, the R/R_{air} ranges from 0.66 to 0.76 in these samples, confirming the presence of small amounts of radiogenic ^{4}He and very low levels of tritiogenic ^{3}He*. Most likely, the loss of gas occurred near the water table because methane concentrations are ~1 atm. Alternatively, CH_4 in the vadose zone may displace a significant percentage of the atmospheric gases dissolved in the water.

Five water samples from some of the relatively deep wells of this study (100–250 m), most of them in the upper aquifer, have an $R/R_{air} < 0.6$ and a moderate concentration of radiogenic helium (>10 μcm^3/kg). To establish approximate groundwater ages for those samples that did not contain tritium,

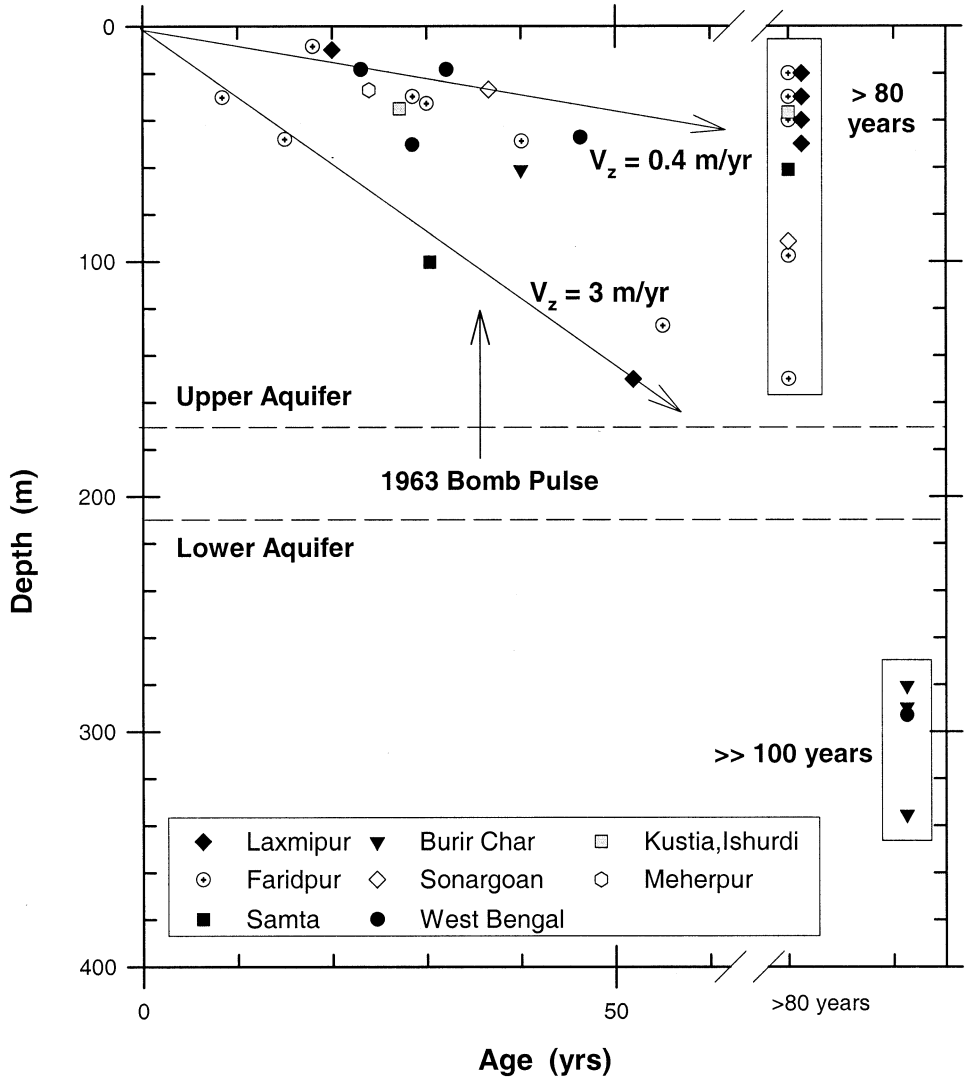

Fig. 2. Groundwater $^3He/^3H$ ages vs. depth in the Bengal Basin. This groundwater age vs. depth plot shows two different vertical velocities within the upper aquifer, suggesting a complicated depositional environment with large variations in sediment permeability. Symbols correspond to sample location sites in Figure 1.

we first examined the release of ^4He from the aquifer sands. The quartz separates of the Laxmipur drill core have low ^4He concentrations (average $^4He = 0.430$ $\mu cm^3/g$) and low $^4He/^{21}Ne$ ratios ($<4 \times 10^6$ compared to the production ratio of 2.5×10^7), indicating a loss between 84 and 99% of the initial ^4He. On the basis of the diffusion rate of He in the quartz and the average ^4He concentration in the groundwater, we estimate an average radiogenic ^4He accumulation rate of 0.02 $\mu cm^3/kg$ water/yr, equivalent to other coastal plain aquifers studied (see Solomon et al., 1996, and Hunt, 2000, for details). Using this accumulation rate, most of the groundwater samples are older than 100 yr. In the lower aquifer (>200 m), the well samples have an $R/R_{air} < 0.4$, indicating a significant amount of radiogenic ^4He. The deepest groundwater samples (Table 1: BGD 23–25, IND 09) have no tritium, a large range of methane concentrations (0.2–173.2 cm^3/kg), and elevated $^4He_{rad}$ levels (>100 $\mu cm^3/kg$), signifying long residence times (>10 times the upper aquifer). The groundwater in the lower aquifer is estimated to be > 1000 yr old, assuming a similar ^4He accumulation rate as in the upper aquifer (Hunt, 2000; Hunt et al., in preparation). High levels of helium and methane in the deepest groundwater are more likely associated with thermogenic natural gas rather than biogenic methane. The dissolved ^4He and CH_4 in the deepest samples are most likely from the upward diffusion of deep natural gas deposits. At Barishal and Burir Char, the $^4He/CH_4$ ratio of 0.0003 in the water samples suggests natural gas deposits of probable early Tertiary age.

4.2. Groundwater Chemistry

The groundwater chemistry (Table 2) of the GBR floodplain is mostly dominated by calcium carbonate with some sodium chloride, no sulfate, and background levels of most trace metals, except Sr, Ba, and As. Several wells at Burir Char and Laxmipur have significantly higher levels of sodium chloride (3–54% seawater), probably caused by seawater intrusion in the

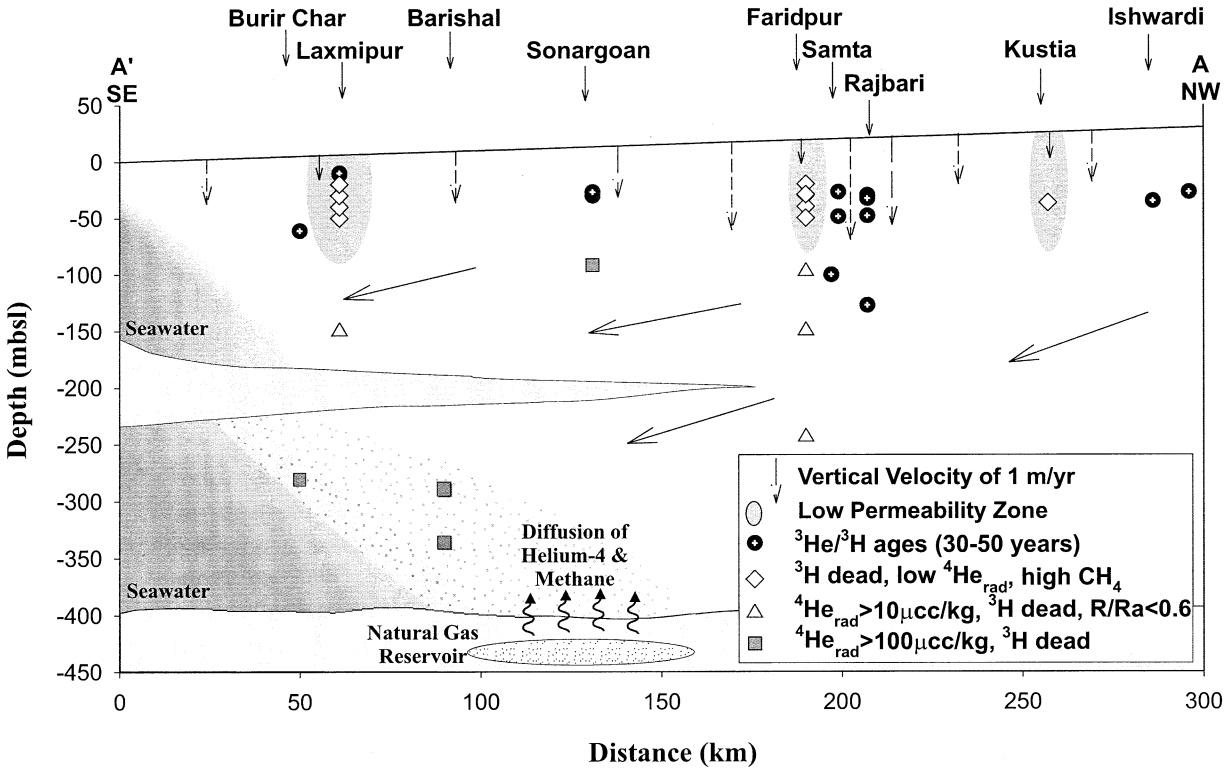

Fig. 3. Schematic cross-section of groundwater flow in the Bengal Basin along the NW-SE (A-A') line. All wells are projected to the A-A' line in Figure 1. There are many municipal wells (up to 150 m) that contain tritium and have a groundwater age. Shallow wells at Laxmipur, Faridpur, and Kustia are tritium dead with high biogenic methane. Deeper wells in the upper aquifer, with no tritium and moderate amounts of radiogenic ^{4}He, are greater than 100 yr old. The recharge in the highly permeable sediments drives the groundwater flow in the lower part of the aquifer. In the lower aquifer, the groundwater has no tritium, elevated methane and helium concentrations, and residence times of greater than 1000 yr. The seawater-freshwater zone is not stagnant and is dominated by ion diffusion and density-driven flow (Carey and Wheatcraft, 1995; Carey et al., 1995; Wheatcraft and Burns, 1997). The lengths of the down-pointing arrows approximate the magnitudes of the vertical velocities.

deepest wells at Burir Char and tidal surge and flooding in Laxmipur. In the groundwater samples, excluding those wells that have probable saltwater contamination (Cl $>$ 170 mmol/L), the average Sr and Ba concentrations are 5.2 $\pm$ 3.4 and 1.3 $\pm$ 1.0 μmol/L, respectively, or $\sim$7 to 9 times the GBR water values (Sr = 0.8 μmol/L, Ba = 0.15 μmol/L) (Dowling et al., 1999). All other trace metal concentrations are at or near the detection limit for V, Ni, Mo, Ag, Cd, Pb, and U (1–100 nmol/L). In all of the wells (except those with saltwater intrusion), the ratios of trace metal concentrations to chloride, including V, Mn, Fe, Ni, Zn, As, Sr, Mo, Ag, Cd, Ba, Pb, and U, are much greater than the seawater ratios, indicating that the dissolved trace metals in the groundwaters are probably derived from the weathering of aquifer protolith rather than from sea spray.

Throughout the Bengal Basin, a positive correlation between groundwater Sr and HCO_3 (excluding seawater intrusion samples) is seen (Table 2, Fig. 4), suggesting that the Sr in the groundwater is being derived from the weathering of carbonates. Another good indicator of the source material for weathering is the ratio of sodium + potassium to chloride. Chloride, as a conservative tracer typically not affected by water-rock interactions, has few sources in groundwater other than sea spray, precipitation, seawater intrusion, or NaCl dissolution. However, sodium + potassium, in addition to the sources noted above for chloride, enter groundwater from the breakdown of Na and K bearing feldspars. Molar ratios (Na + K/Cl) $>$ 1 indicate silicate (feldspar and mica) weathering (e.g., Stallard and Edmond, 1983, 1987), with the magnitude expressed as $(Na + K)_{excess}$ = (Na + K $-$ Cl). As shown in Table 2 and Figure 4, there is an inverse relationship between dissolved Sr and excess Na + K whereby the largest Na and K excess occurs at the lowest Sr concentrations. As Sr increases, excess Na and K decrease, indicating that strontium is not coming from the same source as excess sodium and potassium (e.g., silicate weathering). The inverse trend emphasizes the overall importance of the role of carbonates in the dissolved Sr budget of the groundwater (Table 2, Fig. 4).

Calcium also correlates with strontium and barium, with Ca/Sr ratios in the groundwater of 3 to 6 times the seawater ratio (Fig. 5), even in places such as Laxmipur, where there is clear evidence of seawater flooding and a seawater source for the strontium. This observation suggests that the sediment controls the Sr concentrations via adsorption and desorption reactions. The majority of the groundwater samples have a Ca/Sr ratio of 600 (Fig. 5), verifying that cation exchange and adsorption of Sr are taking place and that Sr is more strongly adsorbed than Ca on the sediment surfaces. Measurements of

Table 2. Bengal Basin groundwater, well depths, major ions, and selected trace metal and isotope data. All concentration data are in μmol/kg.

Sample name	Sample date	Sample location	Depth (m)	Na	NH_4	K	Mg	Ca	Cl	NO_3	SO_4	HCO_3	Fe	Sr	$^{87}Sr/^{86}Sr$	Ba	Excess (Na + K)
BGD 1	May-99	Laximpur	244	3570	104	158	1820	1614	7581	nd	nd	4592	37	6.92	0.715560	1.76	–3853
BGD 2	May-99	Sonapur	11	11,235	459	397	2072	1008	7326	191	160	10,218	14	4.04	0.715376	0.08	4307
BGD 3	May-99	Faridpur	20	2432	273	1162	1569	3457	99	28	nd	12,547	36	5.77	0.721802	1.50	3495
BGD 4	May-99	Faridpur	30	782	313	71	1120	2077	96	nd	5	9628	34	3.75	0.722496	1.05	757
BGD 5	May-99	Faridpur	40	1034	331	90	777	1485	121	nd	2	8676	31	2.74	0.720032	0.91	1003
BGD 6	May-99	Faridpur	150	9548	nd	107	1417	2412	10,635	nd	18	8234	11	7.67	0.717679	0.80	–980
BGD 7	May-99	Faridpur	50	1021	347	116	870	1282	128	nd	nd	6807	38	2.91	0.718465	1.19	1010
BGD 8	May-99	Faridpur	244	4097	287	185	1684	1868	2550	nd	nd	[a]	65	4.89	0.717393	2.09	1733
BGD 9	May-99	Faridpur	98	6355	nd	78	1136	1639	3290	nd	nd	[a]	13	4.04	0.718726	0.99	3143
BGD 10	May-99	Ahladipur	30	376	40	188	1031	2488	769	nd	289	8398	16	4.66	0.723131	1.29	–205
BGD 11	May-99	Rajbari	48	799	nd	96	646	2308	758	nd	22	7774	4	2.28	0.720631	0.77	138
BGD 12	May-99	Rajbari	33	461	nd	77	748	2099	195	nd	5	7791	8	3.18	0.723985	0.57	343
BGD 13	May-99	Rajbari	127	1403	47	189	1653	2983	343	nd	15	4428	47	4.92	0.720017	1.10	1249
BGD 14	May-99	Talma	44	1610	386	351	2601	1326	2669	164	nd	5577	108	4.85	0.721220	1.28	–708
BGD 15	May-99	Nagarkanda	29	924	299	134	1708	3964	2436	1	25	9513	121	7.05	0.722033	1.84	–1377
BGD 16	May-99	Samta	9	2460	166	124	2006	5168	5564	81	nd	13,203	92	8.43	0.727327	5.65	–2980
BGD 17	May-99	Samta	49	801	139	50	1083	2479	793	84	nd	7397	62	4.03	0.726306	2.26	58
BGD 18	May-99	Samta	61	857	146	54	1114	2646	1174	nd	nd	7315	66	4.19	0.727011	2.47	–263
BGD 20	May-99	Jhenidah	100	299	23	50	526	1612	157	nd	1	3936	10	1.96	0.723960	0.84	192
BGD 21	May-99	Burir Char	61	12623	nd	141	621	459	3856	nd	90	11,153	7	1.11	0.714309	0.07	8908
BGD 22[b]	May-99	Burir Char	152	246,020	5400	3549	15,450	2625	295,492	nd	nd	1558	2	26.55	0.710301	2.56	–45,924
BGD 23[b]	May-99	Burir Char	280	267,073	nd	nd	12,012	11,277	257,444	nd	nd	57,405	0	52.74	0.714327	6.59	9628
BGD 24	May-99	Barishal	335	6807	108	57	159	197	2784	nd	nd	[a]	1	1.07	0.714933	0.18	4080
BGD 25	May-99	Barishal	290	6707	86	49	166	188	2051	nd	nd	[a]	1	1.12	0.714462	0.17	4705
BGD 26	May-99	Madaripur	30	783	46	56	1004	2576	815	nd	nd	[a]	85	bdl	0.726818	0.72	25
BGD 27	May-99	Choto Arjundi	27	545	377	135	833	1525	330	1	nd	8857	159	bdl	0.719026	1.05	350
BGD 28	May-99	Mugraoara	a	7160	nd	nd	522	911	4891	nd	40	5412	0	2.43	0.715224	0.08	2269
BGD 29	May-99	Patalpara	a	2273	274	128	893	2786	1008	1	nd	7840	39	4.55	0.720389	0.73	1394
BGD 30	May-99	Adampur	91	6651	nd	82	1020	464	2439	nd	24	[a]	4	1.93	0.712446	0.06	4293
BGD 31	May-99	Laxmipur	50	50,683	1156	523	7454	1427	55,267	nd	nd	11,235	93	14.66	0.717385	2.60	–4061
BGD 32	May-99	Laxmipur	40	52,458	2277	619	5806	4688	65,489	nd	146	6774	111	16.75	0.716232	4.11	–12,412
BGD 33	May-99	Laxmipur	30	50,874	2081	559	5810	5589	63,357	nd	254	8037	140	18.10	0.717253	3.21	–11,923
BGD 34	May-99	Laxmipur	20	29,717	1311	579	5048	4554	38,883	nd	nd	8611	82	15.43	0.715218	2.46	–8586
BGD 35	May-99	Laxmipur	10	12,919	481	290	1478	834	14,251	7	7	4756	14	3.01	0.713317	0.46	–1043
BGD 36	May-99	Laxmipur	150	177,990	nd	1846	23,365	11,527	212,355	nd	4239	3854	57	53.62	0.712724	1.33	–32,519
BGD 37	Jan-00	Shibganj	42	1783	nd	57	1607	3506	312	nd	452	11,609	0	5.30	0.730943	0.84	1529
BGD 38	Jan-00	Nawabganj	9	1105	38	106	1649	4164	1458	nd	166	10,520	72	6.09	0.724952	1.79	–247
BGD 39	Jan-00	Nawabganj	19	1301	374	139	1337	3610	1568	9	nd	8899	75	6.54	0.734896	2.12	–128
BGD 40	Jan-00	Nawabganj	34	982	52	76	1271	3733	981	9	8	9305	58	5.74	0.727071	1.86	77
BGD 41	Jan-00	Iswardi	36	1589	nd	22	1312	2564	67	nd	16	8641	0	3.39	0.717715	0.25	1543
BGD 42	Jan-00	Iswardi	30	1439	nd	21	1626	3214	64	nd	27	11,204	16	5.23	0.719885	0.37	1396
BGD 43	Jan-00	Padma River	33	1906	nd	32	1645	2910	117	nd	46	10,380	23	4.38	[a]	0.58	1821
BGD 44	Jan-00	Baghail Dotala Sako	35	1186	7	23	1053	2863	348	nd	38	8004	1	6.38	0.722089	0.64	861
BGD 45	Jan-00	Baghail Dotala Sako	35	978	8	19	1190	3175	309	nd	4	9762	14	6.85	0.724097	0.83	689
BGD 46	Jan-00	Ruppur	18	217	11	71	890	2424	131	nd	10	7095	6	4.42	0.724460	1.16	157
BGD 47	Jan-00	Meherpur	32	1109	nd	62	838	2958	714	nd	192	7649	0	3.47	0.721440	1.01	457
BGD 48	Jan-00	Refugee Para	27	645	26	70	1351	3140	176	nd	3	8799	7	4.42	0.724011	0.96	539
BGD 49	Jan-00	Ghosh Para	36	686	66	77	1580	4108	2283	nd	641	7730	65	6.32	0.725387	2.25	–1521
BGD 50	Jan-00	Ujjalpur	40	637	50	124	1153	3181	49	nd	2	9125	75	4.92	0.724386	2.00	711
BGD 51	Jan-00	Ghosh & Refugee	36	1310	nd	108	1262	3217	835	nd	56	8729	67	5.31	0.725092	1.91	584
BGD 52	Jan-00	Kustia	33	1913	nd	22	1209	3388	89	nd	3	10,177	13	3.58	0.719646	0.60	1846
BGD 53	Jan-00	Kustia	37	618	69	62	954	2577	175	1	9	7386	72	3.87	0.728289	1.87	504
BGD 54	Jan-00	Kustia	35	755	nd	17	888	2668	119	nd	6	5733	1	3.86	0.725448	0.37	653
BGD 55	Jan-00	Paurosabha	82	1047	10	59	1121	3244	119	nd	1	9177	3	4.69	0.723205	0.62	987
BGD 56	Jan-00	Kustia Town	88	781	68	70	1014	3172	84	18	3	8614	18	4.46	0.722334	0.71	767
IND 1	Jan-00	Moyna	50	826	43	56	1682	3276	[a]	[a]	[a]	[a]	45	7.35	0.724705	0.65	[a]
IND 2	Jan-00	Moyna	114	1880	9	86	1353	1961	[a]	[a]	[a]	[a]	1	6.33	0.721479	1.23	[a]
IND 3	Jan-00	Moyna	47.2	821	nd	44	1253	3043	[a]	[a]	[a]	[a]	0	5.63	0.725555	0.44	[a]
IND 4	Jan-00	Moyna	18.3	451	37	52	944	2636	[a]	[a]	[a]	[a]	57	3.57	0.724236	1.67	[a]
IND 5	Jan-00	Moyna	46	764	64	39	1200	3821	[a]	[a]	[a]	[a]	38	5.41	0.726963	2.01	[a]
IND 6	Jan-00	Birohi	18.3	617	nd	54	1036	2550	[a]	[a]	[a]	[a]	53	4.48	0.724174	2.80	[a]
IND 7	Jan-00	Birohi	126	488	nd	49	691	1849	[a]	[a]	[a]	[a]	11	3.92	0.723347	2.63	[a]
IND 8	Jan-00	Birohi	207	1549	7	61	872	1954	[a]	[a]	[a]	[a]	1	4.70	0.725296	0.65	[a]
IND 9	Jan-00	Baruipur	293	2993	nd	77	1361	1587	582	13	528	8710	4	5.08	0.721128	0.96	2488
DAC 1	Jan-00	Dhaka	[a]	586	nd	26	407	780	[a]	[a]	[a]	[a]	0	2.37	[a]	0.12	[a]
DAC 2	Jan-00	Dhaka	[a]	1485	nd	32	383	657	[a]	[a]	[a]	[a]	0	1.69	0.717620	0.52	[a]
DAC 3	Jan-00	Dhaka	[a]	1172	nd	19	361	605	[a]	[a]	[a]	[a]	11	1.83	0.716398	0.29	[a]
		Averages															
		Total		15,179	416	217	2145	2747	19,250	43	204	9175	36	6.97		1.37	
		w/o BGD 22[b], 23[b], 36[b]		5092	195	136	1451	2479	5900	11	63	8359	37	5.16		1.27	

nd = not detected. bdl = below detection limit.

[a] not available.

[b] Cl > 170 md/L.

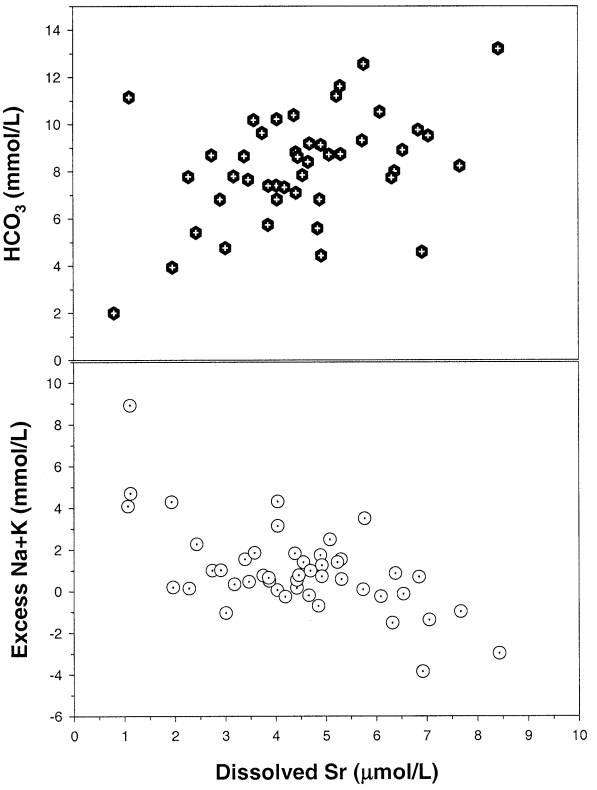

Fig. 4. Bengal Basin groundwater Sr concentrations plotted against HCO_3 and excess Na + K. A positive correlation exists between groundwater Sr and HCO_3 showing that the main source of dissolved Sr in the groundwater is the weathering of aquifer carbonates. Limited silicate weathering is indicated by the inverse relationship between dissolved Sr and excess Na and K. The samples (BGD 22, 23, and 36) that have Cl > 170 mmol/L are excluded.

exchangeable cations in the Laxmipur sediment oxalate extracts confirm that Sr is strongly adsorbed, with a $^{87}Sr/^{86}Sr$ ratio approaching that of seawater and negligible Ca on the exchange sites.

We also observe a positive correlation between groundwater strontium and barium (Fig. 5). The elevated dissolved Ba concentrations in the groundwater and the Ba/Sr ratios being much greater than that of seawater suggest that the groundwater source for Ba is the weathering of the aquifer protolith or desorption from river sediments. The positive trend between Ba and Sr in groundwater and the high values of adsorbed Ba on river sediments imply that adsorption probably controls the Ba and Sr distribution in groundwater. Figure 6 demonstrates that strontium and barium concentrations correlate well with dissolved iron in the Laxmipur groundwater. Because anaerobes are reducing iron oxy-hydroxides (FeOOH) for a source of oxygen in the Bengal Basin groundwaters (Cummings et al., 1999; McArthur et al., 2001; Dowling et al., in press), an additional source of Ba (and some Sr) is the microbial dissolution of FeOOH sediment coatings that had adsorbed Sr and Ba as oxic river sediments.

Figure 7 compares the $^{87}Sr/^{86}Sr$ values to 1/Sr for river water and groundwater samples, demonstrating the control that the sediment source has on the final Sr isotopic composition. The isotopic ratios of the coastal West Bengal ($^{87}Sr/^{86}Sr \approx 0.721–0.727$) and inland Bangladesh groundwater samples ($^{87}Sr/^{86}Sr \approx 0.717–0.735$) are similar to the Ganges River ($^{87}Sr/^{86}Sr \approx 0.724–0.741$), implying that the sediment source is mainly from the Ganges drainage basin. In contrast, the coastal Bangladesh and the Meghna groundwater samples ($^{87}Sr/^{86}Sr \approx 0.710–0.718$) and Brahmaputra and Meghna river samples ($^{87}Sr/^{86}Sr \approx 0.717–0.720$) have similar but lower $^{87}Sr/^{86}Sr$ values compared to the Ganges watershed. The Brahmaputra River is known to carry a higher sedimentary load that ultimately deposits in the coastal portions of Bangladesh. None of the high $^{87}Sr/^{86}Sr$ that dominates the Ganges drainage appears in the coastal groundwaters, which suggests that the coastal Bangladesh sediments were derived from the Brahmaputra River basin.

The strontium isotopes of the Laxmipur groundwater range from 0.71332 to 0.71739 and average 0.71554 ± 0.00173 (Table 4). Strontium isotope ratios increase from shallow to deep, demonstrating the effects of seawater flooding. The Sr isotopic signature of the shallow groundwater represents a complicated mix of seawater Sr ($^{87}Sr/^{86}Sr = 0.7092$) and products of weathering modified by adsorption and desorption reactions. The shallow Bengal Basin groundwater samples (<60 m) not experiencing seawater contamination have a high average $^{87}Sr/^{86}Sr$ value of 0.72363 ± 0.00407.

4.3. Sediment Data and Distribution Coefficients

Deltaic, fluvial, and subsurface sediments have long been shown to have an important buffering effect on the chemistry of the ground and river water for Sr (Cerling and Spalding, 1982; Cerling and Turner, 1982; Johnston and Gillham, 1984; Johnston et al., 1985; Liszewski et al., 2000), but also for Ba, which adsorbs more strongly. To further examine the sources and controlling factors of dissolved Sr and Ba, we measured the adsorbed trace metals on two river sediments and five separate drill core depths (bulk, clay, and mica fractions) from the core sediments. Table 3 shows the Sr and Ba concentrations adsorbed on bulk river sediments (RW-53 and RW-54), Laxmipur bulk core (Lax-depth[m]-B), Laxmipur core fine-grained sediments (Lax-depth[m]-F), and Laxmipur core mica (Lax-depth[m]-M). Table 3 also displays the Sr and Ba data from the digestion of Laxmipur core fine-grained sediments (Lax-depth[m]-F-dig) and mica (Lax-depth[m]-M-dig) after the oxalate extraction procedure. The sediment at 23 and 39 m was devoid of mica. Our ammonium oxalate extraction procedure releases the exchangeable and adsorbed trace elements but did not dissolve the carbonates in the sediments because there was no measurable calcium in the oxalate extracts. Magnesium was the only major cation in the oxalate supernatant (>1 ppm). The high iron concentrations in the supernatant (Table 3) demonstrate that the oxalate extraction dissolved the iron oxy-hydroxides that visibly coated the quartz grains in the sediment.

Because we have both the dissolved and adsorbed trace metal data from one location (Laxmipur, Bangladesh), we are able to investigate the processes that control Sr and Ba concentrations in the groundwater. Figure 8 shows the dissolved HCO_3, Sr, and Ba for the Laxmipur groundwater well cluster (Table 2) and the adsorbed Sr and Ba data for the Laxmipur drill core (Table 3) against depth. The dissolved HCO_3, Sr, and Ba increase with depth to approximately steady state. The bulk

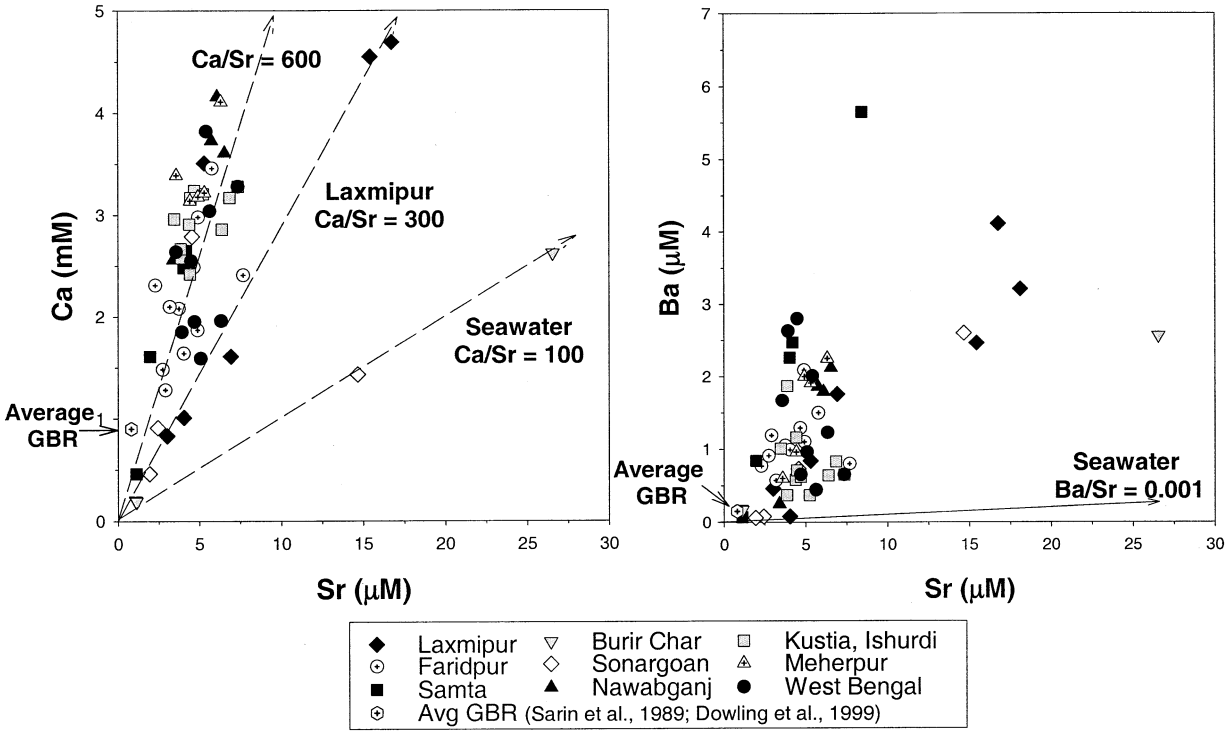

Fig. 5. Relationships among Sr, Ca, and Ba in the Bengal Basin groundwaters. The seawater ratio trends (Ca vs. Sr and Ba vs. Sr) and the average Ganges-Brahmaputra river (GBR) values of Sr, Ca, and Ba are also shown. Note that the GBR values plot at the dilute limit of Ba and Sr concentrations, suggesting that cation exchange and adsorption and desorption reactions on sediments have a strong influence on the concentrations of Sr, Ba, and other trace metals in both the river and groundwater. The Ca/Sr ratios (3–6 times that of seawater) also indicate that Sr is being adsorbed onto sediments. The positive correlation between Ba and Sr as well as the Ba/Sr ratios being much greater than seawater suggests that Ba is more strongly adsorbed than Sr.

sediment and mica separates have similar concentrations for extractable Sr and Ba. However, at a depth of 23 m, there is a small but noticeable decrease in extractable Sr in the bulk sediment and a significant decrease for the fine-grained fraction. The digestion of the fine-grained sediments from the 23-m deep sediment sample (Table 3) shows a considerable decrease in Sr concentration within the sediment, possibly from the loss of structural strontium. In general, for all depths, the fine-grained sediments have much higher extractable concentrations of Sr and Ba (~10 times) because they have a higher surface area/volume ratio and a greater number of exchange sites per gram to adsorb Sr, Ba, and other trace metals. The clay-sized particles, which constitute < 10% of the mass and have the majority of the exchangeable sites for Sr and Ba, appear to control the Sr and Ba concentrations in the groundwater.

The distribution coefficient (K_d) of an exchangeable element is the ratio between the groundwater and aquifer protolith that represents the amount of an element dissolved in the groundwater relative to the amount adsorbed onto the aquifer protolith. It is defined by $K_d = [A]_s/[A]_{eq}$ where $[A]_s$ is the concentration of A adsorbed onto the sediment (in μmol/kg), and $[A]_{eq}$ is the concentration of A dissolved in solution (in μmol/L). In the oxalate supernatant of the river sediments, adsorbed magnesium has an average K_d value of 166 ± 49 mL/g, whereas in the core, the average K_d of Mg is 6 ± 4.5 mL/g. There is no measurable Ca in the oxalate fraction. However, assuming a minimum detection limit of 0.05 ppm (0.0125 mmol/L) for our Dionex ion chromatograph, we estimate the distribution coefficients of calcium at <0.016 ± 0.004 mL/g in the river sediment and <0.005 ± 0.0035 mL/g in the core samples. The main source of dissolved calcium in the groundwater is the weathering of the protolith. Because calcium is not present in the oxalate extracts, the sediment cannot supply Ca to the groundwater by sediment desorption reactions. The strong correlation of calcium and strontium with bicarbonate supports the weathering of carbonates at or near the water table as the dominant Ca and Sr input in the floodplain.

In contrast, the average calculated distribution coefficient of Ba in the river sediments (Tables 2 and 3) is 786 ± 98 mL/g, demonstrating the strong adsorption of Ba onto present-day river sediments. Therefore, river sediments are the likely source of barium in the Bengal Basin. When the sediments become part of the aquifer, the change in environment (redox, bacteria) releases barium through desorption reactions. Throughout the analyzed drill core, the apparent K_d value for Ba decreases with depth. The shallow core (≤20 m) sediments have a barium K_d value of 80 mL/g, whereas in the deeper core (≥20 m), the average value is 16 ± 8 mL/g. In addition, the (Ba/Fe)(×1000) ratios of oxic river sediments (*average bulk* = 7.7 ± 1, *average fine* = 5.7 ± 1) are 6 to 8 times higher than the Laxmipur core. In the Laxmipur sediment samples, the (Ba/Fe)(×1000) ratios of the bulk (average = 1.2 ± 0.5) and fine-grained (average = 1.32 ± 0.6) are fairly consistent with depth. Barium release from the sediment to the groundwater by desorption reactions

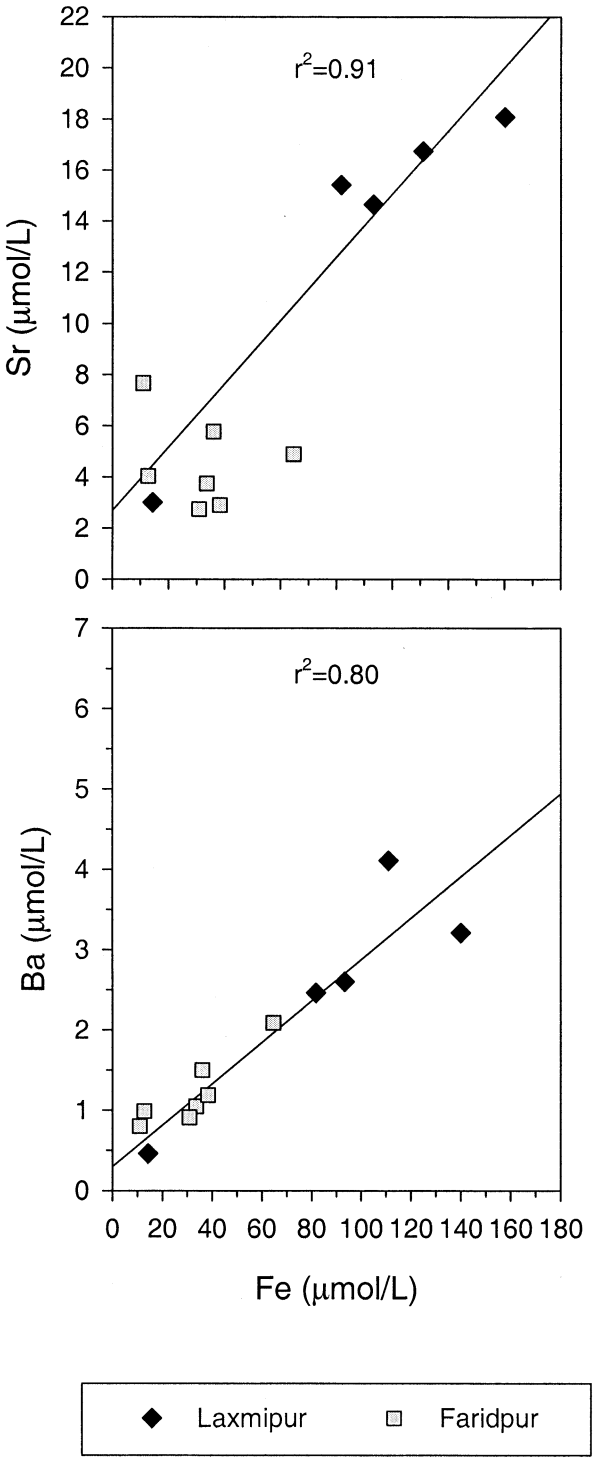

Fig. 6. Dissolved Fe plotted against Sr and Ba. Strontium and barium concentrations correlate well with dissolved iron in the Laxmipur groundwater. Because iron oxy-hydroxides (FeOOH) are being reduced by anaerobic microbes as a source of oxygen in the Bengal Basin groundwaters (Cummings et al., 1999; McArthur et al., 2001; Dowling et al., in press), the microbial dissolution of FeOOH that had adsorbed Sr and Ba as river sediments is another source of Ba (and some Sr) in the river water.

and by the microbial mediated brea$K_d$own of FeOOH are the most reasonable explanations.

Another suggested source of dissolved barium is from the weathering of barite ($BaSO_4$). However, barite was not found in either our XRD analyses of the Laxmipur core or GBR floodplain sediments; there is also no correlation found between Ba and SO_4, and the concentrations of barium are greater than sulfate in most samples. Most of the groundwater samples are undersaturated with respect to barite, except for the few samples (BGD 32, 33, and 36) collected from an area experiencing seawater flooding (Laxmipur). The average Ba values (1.3 ± 1.0 μmol/L) for the groundwater exclude those wells that have probable saltwater contamination (Cl $>$ 170 mmol/L), such as Laxmipur. There is no evidence of sulfate reduction in the aquifer because the Eh values are well above the SO_4/H_2S transition (but close to the Fe^{3+}/Fe^{2+} transition), and H_2S was not observed in the field or measured in dissolved gases of the groundwater samples. Cummings et al. (1999), Dowling et al. (in press), and McArthur et al. (2001) showed that anaerobic microbes are reducing iron oxy-hydroxides as an alternative electron acceptor in the absence of oxygen in the Bengal Basin anoxic groundwaters. Barium concentrations correlate well with iron dissolved in the Laxmipur groundwater (Fig. 6) and adsorbed onto fine-grained sediments, suggesting that Ba may be also from the microbial dissolution of iron oxy-hydroxide sediment coatings that had adsorbed large quantities of Ba as oxic river sediments in addition to desorption reactions.

For strontium, a different scenario emerges from our chemical data (Tables 2 and 3). Only trace amounts of Sr are adsorbed onto the river sediments, and thus, the simple desorption mechanism, used above for Ba, cannot explain the elevated Sr observed in the groundwater. The river and core sediments have similar strontium distribution coefficients. The average riverine K_d value for Sr is 7 ± 2 mL/g, whereas the shallow core ($\leq$20 m) has a strontium K_d of 14.3 mL/g, and the deeper core ($\geq$20 m) has an average K_d of 1.6 ± 0.7 mL/g. The calculated Sr K_d values for the Laxmipur bulk core and the river sediment fall in the lower range of the measured literature values (1.3–275) (Cerling and Spalding, 1982; Johnston and Gillham, 1984; Johnston et al., 1985; Liszewski et al., 2000). Although the river and core sediments have comparable K_d values, the bulk sediments and mica separates have 5 times more extractable strontium, and the clay-sized particles have 30 times more extractable strontium compared to the river sediments.

Even though the origin of the dissolved Sr in the Laxmipur groundwater is most likely from tidal flooding, sediment adsorption and desorption reactions control the final dissolved Sr concentration. In areas removed from seawater flooding, carbonate dissolution and silicate weathering are the only reasonable sources of Sr in the groundwater, whereas Ba addition occurs by desorption from the sediment (Table 3). The bulk core sediment and the mica separates have comparable amounts of adsorbed Sr and Ba. The digested mica (after the oxalate extraction) contains large quantities of structural Sr and Ba (1–2 mmol/kg), and small amounts of biotite weathering can provide an additional source of Sr and Ba to the groundwater. The fine-grained sediments have high levels of adsorbed Sr and Ba but have lost some of their structural Sr and Ba through weathering. Even though the silicate and carbonate weathering

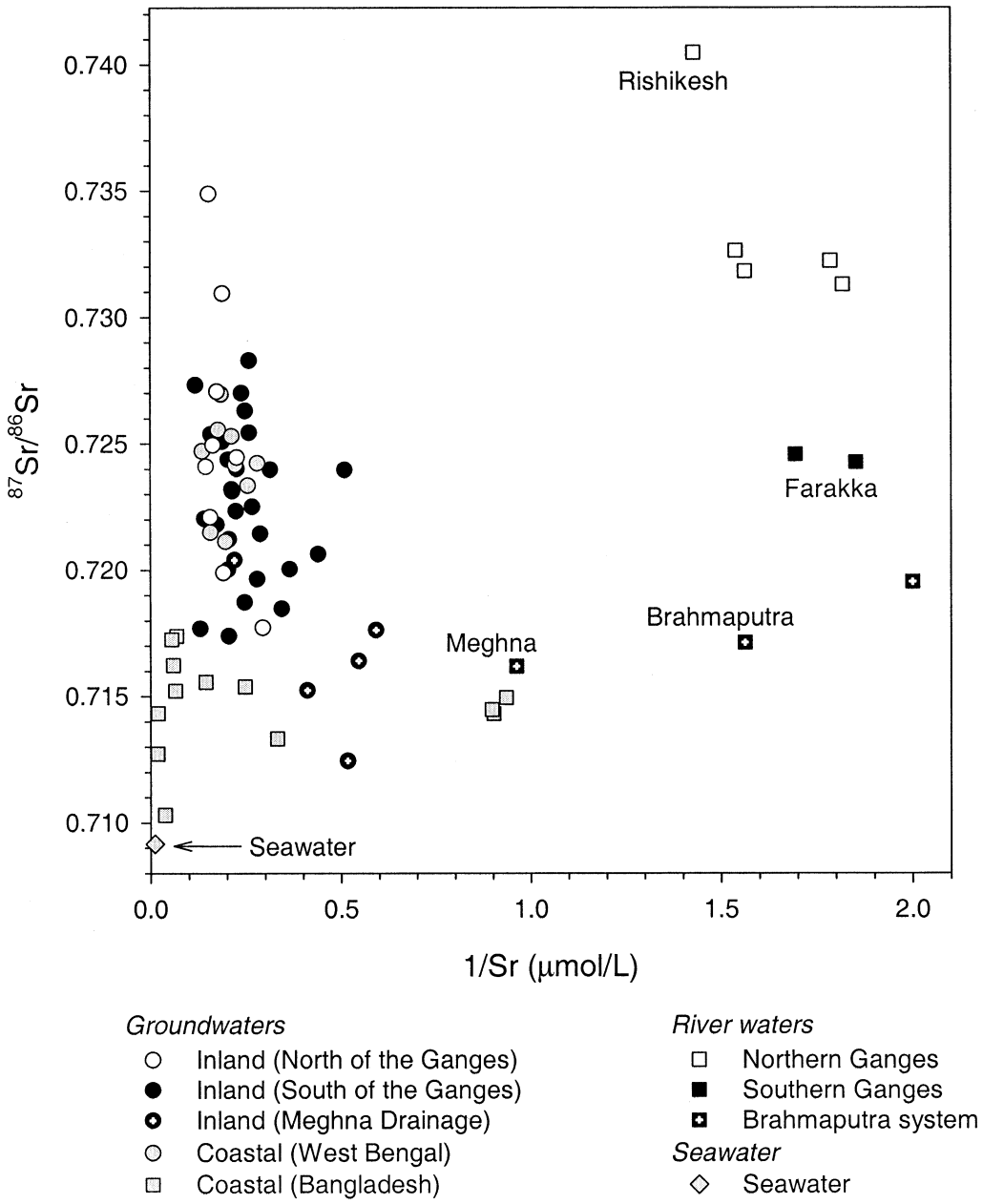

Fig. 7. Groundwater and river water $^{87}Sr/^{86}Sr$ ratios plotted against 1/Sr. The isotopic ratios of the coastal West Bengal and inland Bangladesh groundwater samples are similar to that of the Ganges River, implying that the sediment source is from the Ganges drainage basin. The coastal Bangladesh groundwater samples and Brahmaputra River system have comparable $^{87}Sr/^{86}Sr$ values, which suggests that the coastal Bangladesh sediments were derived from the Brahmaputra watershed.

are sources of dissolved Sr and Ba, sediment adsorption and desorption reactions on the fine-grained sediments control the final Sr and Ba concentrations in the groundwater.

The Sr isotopic measurements of the sediment extractions are displayed in Table 4. There is some variation in the sediment extraction $^{87}Sr/^{86}Sr$ values throughout the GBR floodplain. The sediments not affected by seawater (e.g., river samples) have high exchangeable Sr isotopic values. The average $^{87}Sr/^{86}Sr$ value of the Ganges sediment oxalate extractions ($n = 4$) throughout the watershed is 0.73167 ± 0.01390 (range 0.72271–0.75238), which is greater than the average Ganges River water ratio of 0.72458. The oxalate extraction of the Brahmaputra bulk river sediment ($n = 2$) has an average $^{87}Sr/^{86}Sr$ value of 0.72778 ± 0.00584, which is higher than the average Brahmaputra River water value (0.71712).

The constant seawater flooding of Laxmipur heavily influences the $^{87}Sr/^{86}Sr$ signature of the coastal sediment. In Laxmipur, the $^{87}Sr/^{86}Sr$ average of the bulk sediment oxalates is 0.71202 ± 0.00288, ranging from 0.71013 to 0.71628, and the values are equivalent to the values of the Laxmipur core mica

Table 3. Results of the sediment oxalate extractions and sediment digestions.

Sample		Oxalate extractions											K_d values			Microwave digestion			
Name	Depth (m)	Bulk (μmol/kg [ppm])			Bulk (mmol/kg)	Fine grained (μmol/kg [ppm])			Fine (mmol/kg)	Mica[a] (μmol/kg [ppm])		Mica (mmol/kg)	Bulk [b] (mL/g)			Fine grained (μmol/kg [ppm])		Mica (μmol/kg [ppm])	
River		Mg	Sr	Ba	Fe	Mg	Sr	Ba	Fe	Sr	Ba	Fe	Mg	Sr	Ba	Sr	Ba	Sr	Ba
RW 53	0	29,924	7.3 [0.64]	107.4	15.9	bdl	17.4 [1.52]	352.9	54.8	[c]	[c]	[c]	131.8	9.1	716.2	70 [6]	276	[c]	[c]
RW 54	0	82,398	4.7 [0.41]	128.3	15.0	bdl	7.2 [0.63]	183.1	37.4	[c]	[c]	[c]	201.0	5.8	855.1	121 [11]	425	[c]	[c]
Core		Mg	Sr	Ba	Fe	Mg	Sr	Ba	Fe	Sr	Ba	Fe	Mg	Sr	Ba	Sr	Ba	Sr	Ba
LAX 3	3	21,889	38.2 [3.35]	28.6	23.3	bdl	210.5 [18.44]	118.4	93.8	24.7 [2.16]	46.7	53.7	[d]	[d]	[d]	1704 [149]	2296	1367 [120]	1106
LAX 14	14	18,729	43.2 [3.79]	37.3	22.7	bdl	251.7 [22.06]	149.6	68.2	24.7 [2.16]	34.9	63.6	12.0	14.3	80.5	621 [54]	560	2054 [180]	1557
LAX 23	23	25,888	16.1 [1.41]	55.5	43.1	73,442	33.4 [2.93]	153.4	143.1	[c]	[c]	[c]	4.9	1.0	22.5	234 [21]	621	[c]	[c]
LAX 39	39	6451	25.2 [2.21]	27.8	17.8	bdl	164.8 [14.44]	155.9	98.4	[c]	[c]	[c]	1.0	1.5	6.8	943 [83]	1276	[c]	[c]
LAX 48	48	38,971	34.1 [2.99]	46.1	103.5	bdl	166.8 [14.62]	224.7	472.7	24.9 [2.18]	35.3	95.3	5.2	2.3	17.8	759 [67]	1576	1669 [146]	2142

[a] The mica supernatants were not analyzed for major cations.
[b] Used average Ganges-Brahmaputra river surface and corresponding Laxmipur groundwater concentrations to calculate distribution coefficients.
[c] Either no mica or not enough mica for extractions.
[d] No water data available (above groundwater table).
bdl = below detection limit.

Table 4. Strontium isotopic results of water and sediment oxalate extractions in the Laxmipur groundwater and core samples, Ganges-Brahmaputra (GBR) river water and sediment, and seawater.

Sample	Depth (m)	$^{87}Sr/^{86}Sr$	Sr (μmol/L)
Laxmipur groundwater			
BGD 35	10	0.713317	3.01
BGD 34	20	0.715218	15.43
BGD 32	40	0.716232	16.75
BGD 31	50	0.717385	14.66
Average		0.715538	12.46
Laxmipur core			
Lax 14B	14	0.710454	43.24
Lax 23B	23	0.716277	16.11
Lax 39B	39	0.710128	25.20
Lax 48B	48	0.711220	34.14
Average		0.712020	29.67
Laxmipur mica separates			
Lax 3M	3	0.711741	24.69
Lax 48M	48	0.712075	24.87
Average		0.711908	24.78
GBR water			
Gangesa		0.724580	0.59
Farakka		0.724265	0.54
Ayodhya		0.732237	0.56
Bithur		0.731298	0.55
Garmukteshwar		0.731829	0.64
Rishikesh		0.740480	0.70
Haridwar		0.732649	0.65
Brahmaputra[a]		0.717120	0.64
Meghna		0.716180	1.04
Dhaleshwari		0.719520	0.50
GBR bulk sediments			
Ganges average		0.731667	4.34
Brahmaputra average		0.727780	2.74
Seawater Average		0.70916[b]	91.3[c]

[a] Basu et al. (2001).
[b] Palmer and Edmonds (1989).
[c] Richter et al (1992).

separate extractions ($n = 2$, *average* $= 0.71191 \pm 0.00024$). The $^{87}Sr/^{86}Sr$ compositions of the Laxmipur core sediment and mica separates are similar but lower than the shallow Laxmipur groundwater (0.71554 ± 0.00173). The original high sediment strontium isotopes are diluted and replaced by the lower seawater values via cation exchange.

5. DISCUSSION

As in most hydrologic systems, including our study area in the Bengal Basin, precipitation (>2 m/yr) will follow, to varying degrees, these three paths: evapotranspiration to the atmosphere, runoff to the rivers, and recharge to the aquifer. Groundwater from the shallow part of the aquifer (<20 m) also will contribute water by discharging to the broad and shallow GBR, where the average depth is 13 ± 3 m and varies between 8 and 19 m (Coleman, 1969). However, in the GBR floodplain, groundwater below 30 m does not discharge to the rivers but rather forms the majority of the subsurface discharge throughout the floodplain. We know that this occurs in the floodplain because groundwater age increases with depth in combination with a very low horizontal water table gradient and a rapid vertical velocity (groundwater recharge). For submarine discharge in the Bengal Basin, we envision a two-cell simple box model ($500 \times 500 \times 0.200$ km), as shown in Figure 9. The upper cell is ~30 m deep, with a small percentage of the recharge flowing into the GBR (not shown). Once the water reaches the lower cell (>30 m), the recharge must be balanced by discharge into the coastal oceans. The groundwater recharge rates based on the $^{3}He/^{3}H$ ages in the Bengal Basin (young groundwater ages at depth) demonstrate that the recharge occurs quickly and that groundwater recharged below 30 m does not supply the GBR with any significant amount of water. If little or no recharge occurred, as in the low permeable tills of North America, the $^{3}He/^{3}H$ ages would increase rapidly with depth. However, in highly conductive floodplain sediments, recharge tends to be rapid and is often 20 to 40% of total precipitation (e.g., Fetter, 1988).

In this study, to establish the groundwater flux to the ocean, we use our estimate of travel times for groundwater below 50 m. By using the average recharge rate (60 ± 20 cm/yr) and surface area of the Bengal Basin, we assume a steady-state system in which flux in (recharge) equals flux out (subsurface discharge):

$$\text{Surface Area } (m^2) \times \text{Rechagre Rate (m/yr)} = \text{Submarine Discharge } (m^3/yr).$$

This calculation gives an annual subsurface discharge from Bengal Basin to the Bay of Bengal of $1.5 \pm 0.5 \times 10^{11}$ m^3/yr, or ~15% of the surficial GBR flux to the Bay of Bengal. The average strontium and barium groundwater concentrations (Table 2) are used to determine total groundwater fluxes of Sr ($8.2 \pm 2 \times 10^8$ mol/yr) and Ba ($1.5 \pm 0.3 \times 10^8$ mol/yr), which are comparable to the estimated surface GBR flux of Sr (8×10^8 mol/yr) and Ba (1.5×10^8 mol/yr) to the oceans. The submarine discharge of calcium, a product of silicate and carbonate weathering throughout the Himalayas and the Bengal Basin, is $3.7 \pm 1 \times 10^{11}$ mol/yr, similar to the GBR surface flow into the Bay of Bengal (5.2×10^{11} mol/yr) (Sarin et al., 1989). The actual GBR calcium, strontium, and barium values vary seasonally and inversely with the river discharge (Sarin et al., 1989; Moore, 1997; Galy et al., 1999) because the GBR is a very dynamic system. Our estimate of river flux for Sr differs from that of Richter et al. (1992) (1.3×10^9 mol/yr) because we use a lower Sr river concentration (sampled in January 1999) in our calculations (Dowling et al., 1999). However, it is consistent with the seasonally weighted flux of Galy et al. (1999) (6.5×10^8 mol/yr). Table 5 summarizes the results of the GBR and groundwater discharge and fluxes. One important assumption in our calculations is that the Bengal Basin groundwater hydrology is in steady state. Although short-term transient hydrophenomena can occur, the use of groundwater ages average recharge over several decades. When highly conductive sediments are perturbed, they return to steady-state conditions in < 1 yr. We also attempted to estimate the recharge rate and major and trace ion concentrations over a wide geographic part of the Bengal Basin, in both Bangladesh and West Bengal, India.

Our estimated groundwater flux for Ba agrees with the

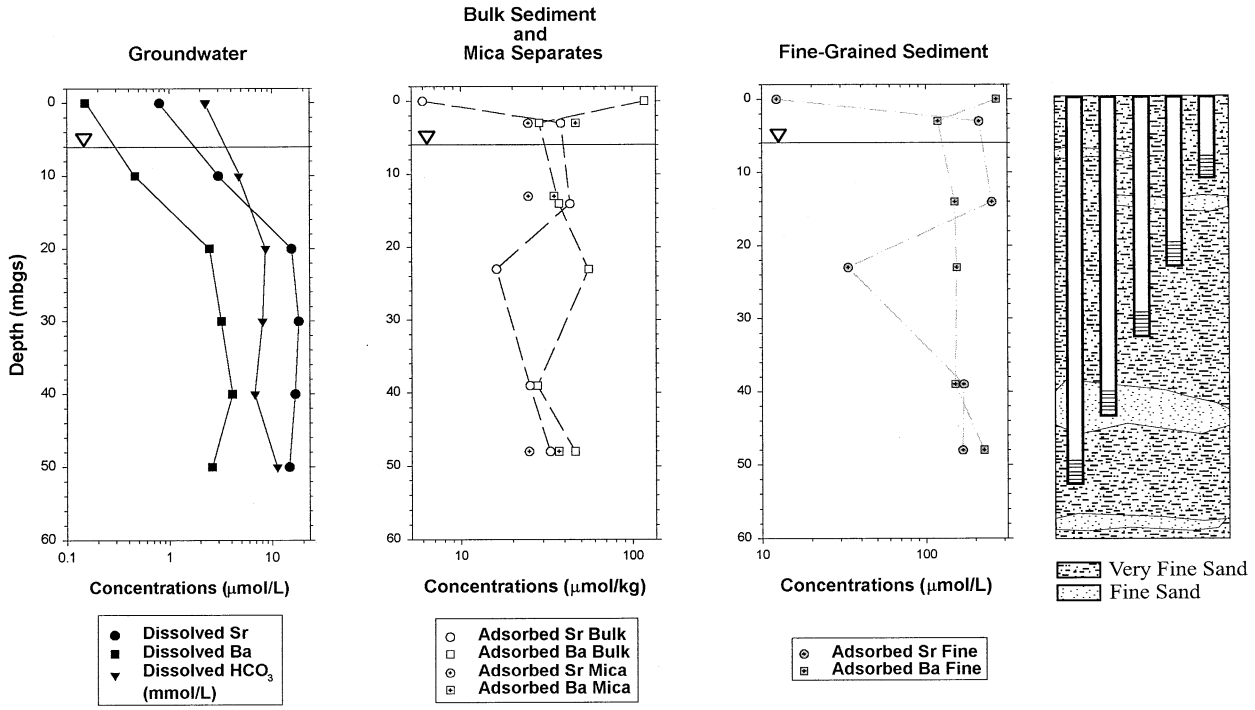

Fig. 8. Groundwater and sediment oxalate extraction data plotted against depth at Laxmipur, Bangladesh. All data are in μmol/kg with the exception of bicarbonate (mmol/kg). Dissolved bicarbonate, strontium, and barium increase with depth to approximately steady-state concentrations. The high concentration of adsorbed Ba on the river sediments suggests that barium can be supplied to the groundwater through sediment desorption. Lower Sr concentrations in river sediments reveal that Sr must be continuously supplied to the groundwater by aquifer protolith or seawater. The exchange and adsorption and desorption of Sr and Ba on sediments control the final river and groundwater concentrations. The sediment cross-section is based on grain size analysis. The diagram shows a coarser interval at 39 m (fine sand; ~0.2 mm), with less than 5% silt. All other core samples were very fine sand (>60% between 0.2 and 0.07 mm), with ~25% silt.

estimate of Moore (1997) (3×10^8–3×10^9 mol/yr), on the basis of measured Ba and ^{226}Ra excesses in the Bay of Bengal. The fact that our Ba estimates fall just below the low end of Moore's (1997) range suggests that our estimated groundwater discharge and trace metal fluxes are not severely overestimated. The Bay of Bengal samples of Moore (1997) were taken during low river flow, allowing him to observe the Ba excess in the Bay of Bengal. His Ba flux estimate can be extrapolated to the full year because the groundwater discharge is fairly constant throughout the year. A simple correlation does not exist between river discharge and groundwater discharge, because the discharge at the seawater-freshwater-groundwater interface is dominated by density driven flow and ion diffusion (Carey and Wheatcraft, 1995; Carey et al., 1995; Wheatcraft and Burns, 1997). Figure 9 illustrates groundwater discharge, the seawater-freshwater interface, and the seawater wedge. As the fresh groundwater flows over the denser underlying seawater, a transition zone is created and controlled by mechanical dispersion, molecular diffusion, and sediment permeability. The velocity of the fresh groundwater increases as it approaches the coastline because the same volume of the freshwater is flowing through a smaller area. Only a small portion of the groundwater flowing above the saltwater wedge interacts with it to create a transition zone, while the majority of the fresh groundwater discharges directly into the coastal oceans. The freshwater-saltwater mixing zone is dominated by density-driven flow, as shown in Figure 9, and the small amount of fresh groundwater that is actually interacting with the saltwater wedge will still discharge into the coastal oceans. The freshwater-seawater transition zone does not affect our estimate for the annual subsurface discharge from Bengal Basin to the Bay of Bengal ($1.5 \pm 0.5 \times 10^{11}$ m^3/yr), which is based on the ^{3}He/^{3}H recharge rate. In addition, our submarine flux estimates are independent of seasonality because they are based on the long-term "average" groundwater recharge and the average dissolved Sr and Ba concentrations.

However, there are many reactions occurring (e.g., precipitation, dissolution, speciation changes, etc.) in the freshwater-seawater transition zone from the changes in pH, redox, and chemistry that may affect and ultimately reduce our calculated fluxes to the marine system for Sr and Ba. Unfortunately, this present data set cannot resolve the myriad of possible reactions that are occurring in the mixing zones (e.g., barium precipitation as barite or adsorbed onto iron oxy-hydroxides), because we have collected very few groundwater samples and no sediment samples from the freshwater-seawater interface. Two groundwater samples (BGD 22 and 23, Burir Char), which are most likely taken from the seawater-freshwater transition zone, have very distinct chemistry: pH > 9; chloride > 45% seawater Cl; no measurable sulfate; and high levels of barium, magnesium, and calcium. Any seawater sulfate must have precipitated or reacted in the saltwater wedge before entering the transition

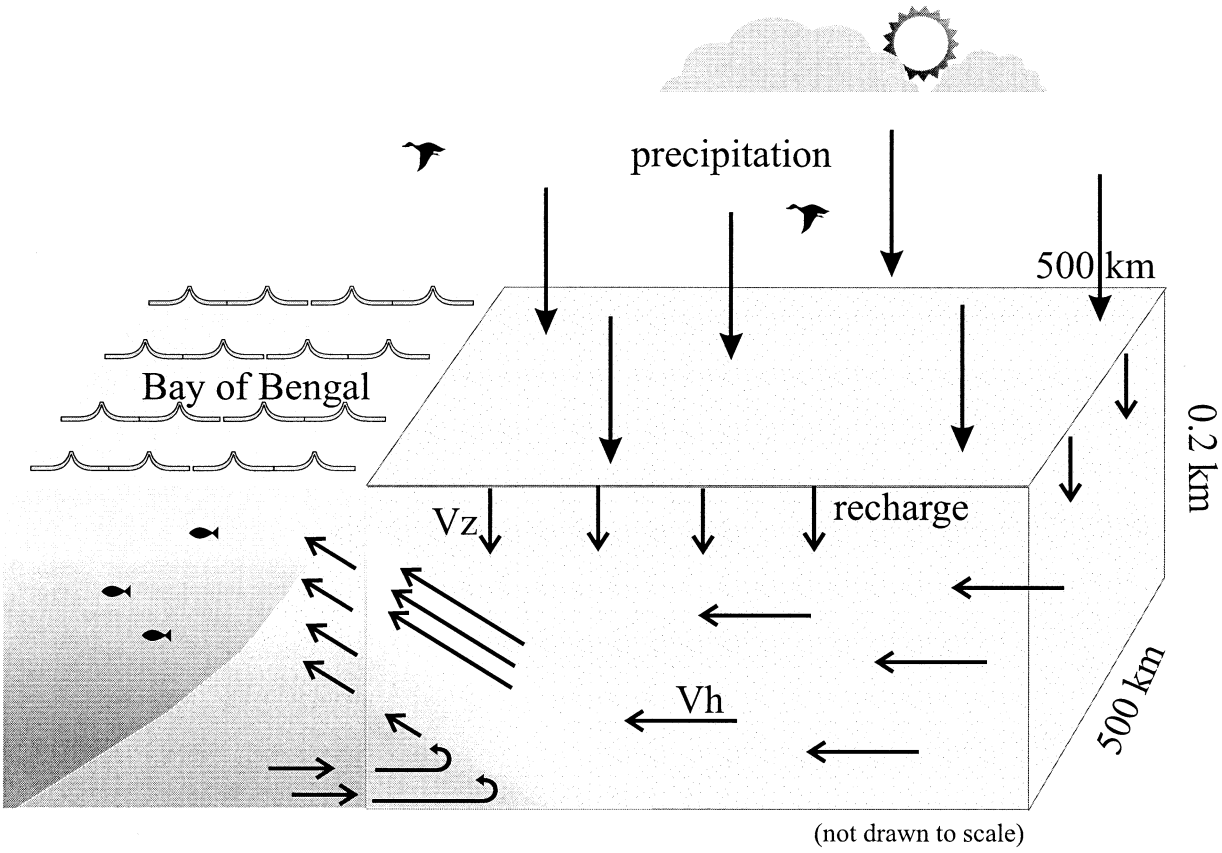

Fig. 9. Submarine discharge into the Bay of Bengal. A box can represent our steady-state groundwater discharge model, with recharge flowing through the top (500 × 600 km) of the box (a footprint of the Bengal Basin) to the aquifer. Once the recharge reaches the aquifer (below 30 m depth), it must be balanced by discharge into the coastal oceans out of the side of the box (~200 m depth). As the fresh groundwater flows past the denser underlying seawater, mechanical dispersion, molecular diffusion, and sediment permeability create a freshwater-seawater transition zone and enhance discharge. The velocity of the fresh groundwater increases as it approaches the Bay of Bengal because the same volume of the freshwater is flowing through a smaller cross-sectional area.

zone. The sulfate reduction is most likely not occurring in the transition zone because H_2S was not observed in the field or measured in the dissolved gases of the groundwater samples.

Our calculated Ca, Sr, and Ba submarine fluxes to the Bay of Bengal are 2.8, 3.3, and 1.2%, respectively, of the total discharge received by the global oceans, which would make significant contributions to the global oceanic budget for calcium, strontium, and barium. However, many floodplains have "soft" groundwater, dominated by Na, K, and low carbonate and do not have substantial dissolved calcium (e.g., Amazon, Alabama, Georgia). The submarine discharge from those aquifers will not significantly increase the Ca or Sr flux to the oceans.

Given the radiogenic $^{87}Sr/^{86}Sr$ ratio of the groundwater, the subsurface discharge makes an even more significant contribution to the rise of the ocean's $^{87}Sr/^{86}Sr$ ratio through the late Cenozoic (Chaudhuri and Clauer, 1986; Basu et al., 1999; Basu et al., 2001) than the surface GBR flux alone. Past modeling has been done with only riverine fluxes and has not taken into account submarine discharge (e.g., Palmer and Edmond, 1989; Galy et al., 1999). Groundwater discharge from the GBR coastal floodplain could account for at least part of the large shift in the marine Sr isotopic data set over the past 40 Ma. Using the groundwater flux estimates developed in this paper, Basu et al. (2001) estimated that the GBR floodplain could contribute 0.82 to 1.86 × 10^{-4} Ma^{-1} to the global strontium isotopic balance. These results show that groundwater discharge can heavily influence the seawater Sr isotopic balance.

To explain this substantial flux of Sr to the oceans from the GBR floodplain and its impact on the Cenozoic evolution of the oceanic $^{87}Sr/^{86}Sr$ ratio, we envision a multistage process of weathering and erosion that begins in the high Himalayas and ends with the riverine and subsurface discharge into the Bay of Bengal. The sediment from the physical weathering of the Himalayas is deposited in the Ganges-Brahmaputra floodplain. Little chemical weathering occurs at the high elevations, and rapid transport of sediment to the floodplain will minimize the effects from chemical weathering. The Food and Agriculture Organization (1971) described the floodplain soils as a combination of clays, quartz, calcium carbonate, dolomite, and mica. Our investigation shows that the sediment core (depth 50 m) from Laxmipur is dominated by quartz, with a considerable amount of biotite, partially altered to vermiculite. The juvenile character of the floodplain sediments, as documented by several

Table 5. Summary of Ca, Sr, and Ba flux for surface and groundwater discharge from the Ganges-Brahmaputra floodplain. The samples affected by saltwater intrusion were not used in calculating the groundwater submarine flux of Ca, Sr, and Ba.

Ganges-Brahmaputra river discharge to the Bay of Bengal	1×10^{12} m^3/yr[a]
Ganges-Brahmaputra river flux of calcium	5.2×10^{11} mol/yr[b]
Ganges-Brahmaputra river flux of strontium	8×10^{8} mol/yr[c]
Ganges-Brahmaputra river flux of barium	1.5×10^{8} mol/yr[c]
Groundwater Submarine discharge to the Bay of Bengal	$1.5 \pm 0.5 \times 10^{11}$ m^3/yr[d]
Groundwater Submarine flux of calcium	$3.7 \pm 1 \times 10^{11}$ mol/yr[d]
Groundwater Submarine flux of strontium	$8.2 \pm 2 \times 10^{8}$ mol/yr[d]
Groundwater Submarine flux of barium	$1.5 \pm 0.3 \times 10^{8}$ mol/yr[d]

[a] Subramanian (1979).
[b] Sarin et al. (1989).
[c] Dowling et al. (1999).
[d] This study.

studies (e.g., Uddin and Lundberg, 1998), suggests that minor chemical weathering has taken place at higher altitudes in the Himalayas, as one might expect from the low temperatures and slow vegetation growth. Many studies have demonstrated the radiogenic Sr signature of the immature sediment (Derry and France-Lanord, 1996; Quade et al., 1997; Galy et al., 1999; English et al., 2000) (Table 4). These same sediments, upon reaching the Ganges-Brahmaputra floodplain, encounter significant plant and bacterial respiration. Respiration produces carbon dioxide and organic acids increasing the pCO_2 in the groundwater and leading to significant carbonate dissolution and some silicate weathering.

It is important to consider the magnitude and dominance of silicate and carbonate weathering in the GBR floodplain because of the long-term effect silicate weathering has on the climate from the consumption of carbon dioxide. Even though several studies have suggested that the floodplain is an important site for silicate weathering (Derry and France-Lanord, 1996; Galy and France-Lanord, 1999), the GBR floodplain is dominated by carbonate weathering, both calcite and dolomite, as shown by the groundwater chemistry. Carbonate dissolution does not affect atmospheric CO_2 at the million-year time scale, because the CO_2 that is used to weather carbonates returns to the atmosphere after oceanic carbonate precipitation. The weathering of carbonates generates the elevated bicarbonate values that range from 4000 to 13,000 μmol/L and average 8400 $\pm$ 2000 μmol/L in the groundwater. Using the same calculation for groundwater flux of Ca, Sr, and Ba, we estimate that $1.3 \pm 0.7 \times 10^{12}$ mol/yr of bicarbonate enters into the oceans. If this estimate were extrapolated to all coastal aquifers, then the net effect would be a short-term sequestration of added atmospheric CO_2 and a substantial and unaccounted sink for carbon at the millennia time scale.

In all Bengal Basin groundwater samples, the bicarbonate ion is balanced by calcium and magnesium (average $Ca + Mg/HCO_3 = 0.9$) from the shallowest (10 m) to deepest (400 m) parts of the aquifer. There is a positive correlation between dissolved Sr and bicarbonate throughout the Bengal Basin (excluding seawater intrusion samples), reinforcing carbonate weathering as an important source of strontium in these deltaic groundwater samples. The positive trend is not based on depth or age but most likely on the heterogeneous geology of the floodplain. The sources of magnesium in the groundwater are dominantly from dolomite dissolution, with minor biotite weathering.

Excess Na and K places limits on the extent of silicate weathering that occurs in the Ganges-Brahmaputra floodplain. Excluding samples with $>$ 170 mmol/L chloride (BGD 22, 23, and 36), excess sodium and potassium (average $[Na + K]/Cl = 5.1$ mmol/L, average $[Na + K] - Cl = 1.8 \pm 2$ mmol/L) values do support some albite (Na), orthoclase (K), and mica (K) weathering in the groundwater. Thus, in some waters, silicate may be important but typically represent $<$ 20% of the total weathered material. We have confirmed by XRD analysis and by visual identification that biotite exists as unweathered, detrital flakes in the river sediments, but many flakes have been altered to vermiculite in the sediment. The strong cation exchange properties of vermiculite suggest the importance of phyllosilicates in silicate weathering because there is only a minor amount of feldspar in the drill core. The magnitude of mica weathering is limited by potassium excess in the groundwater, which ranges from 2 to 241 μmol/L, with an average of 17 μmol/L, or $<$ 5% of the total weathered material. The fact that the dissolved Sr and excess Na + K plot (excluding the saltwater-contaminated samples) shows an inverse relationship (Fig. 4) signifies limited silicate weathering and widespread carbonate weathering. This inverse relationship establishes the dominant source of strontium in the groundwater of the Bengal Basin to be carbonate dissolution, not silicate weathering (Fig. 4).

Several authors have used relative proportions of silicate and carbonate weathering to help determine the $^{87}Sr/^{86}Sr$ ratios of the world's rivers and the ocean through time (Krishnaswami et al., 1992; Palmer and Edmond, 1992; Derry and France-Lanord, 1996; Quade et al., 1997; Blum et al., 1998; Singh et al., 1998; Galy et al., 1999; English et al., 2000). Galy et al. (1999) showed that the bed-load carbonates of the GBR in Bangladesh are sufficiently radiogenic (0.718–0.749) to be the source of radiogenic ^{87}Sr in the groundwater. Alternatively, trace amounts of high-Rb silicate phases would affect the $^{87}Sr/^{86}Sr$ ratio dramatically without changing the total strontium. The ultimate control on the Sr isotopic composition is most likely a complicated combination of carbonate weathering supplying the bulk of the Sr and perhaps the high $^{87}Sr/^{86}Sr$ values. However, we cannot rule out that minor silicate weathering may provide the radiogenic Sr and that sediments buffer the Sr concentration and isotopic ratios via cation exchange and adsorption and desorption reactions. Figure 7 demonstrates that the strongly radiogenic Himalayan headwaters of the Ganges are not observed in the Bengal Basin groundwaters (inland or coastal), because of additional carbonate weathering, cation exchange, and adsorption and desorption reactions in the floodplain sediments. Another possible cause for the lower Sr ratios in the coastal groundwaters is seawater flooding and the fact that the carbonates derived from the Brahmaputra drainage are less radiogenic than those from the Ganges. Thus, the coastal groundwater chemistry and isotopic ratios reflect the Brahmaputra drainage system, whereas the inland waters reflect the

Table 6. Estimated groundwater flux of select trace metals from the Ganges-Brahmaputra river floodplain.

Select trace metals	Mn	Ni	Zn	As	Ag	Pb	U
Groundwater average (μmol/L)	10.546	0.033	3.531	2.239	0.004	0.011	0.005
Submarine discharge (mol/yr)	1.6×10^9	5.0×10^6	5.3×10^8	3.4×10^8	5.3×10^5	1.7×10^6	6.8×10^5
Ocean average (mol)	7×10^{12}	1.1×10^{13}	8.4×10^{12}	3.2×10^{13}	3.5×10^{10}	1.4×10^{10}	1.8×10^{13}
Present τ in the ocean (yr)	1.3×10^3	8.2×10^3	5.1×10^2	3.9×10^4	3.5×10^2	8.1×10^1	5×10^5
Percentage of submarine flux (%)	29.4	0.4	3.2	40.7	0.5	1.0	1.9

more radiogenic metacarbonates of the Ganges drainage (Fig. 7). The Brahmaputra drainage, whose sediment load is much greater than that of the Ganges, may control the final $^{87}Sr/^{86}Sr$ ratio of groundwater discharged to the Bay of Bengal at $\sim$0.716.

A comparison of our sediment extraction data to that of Galy et al.'s (1999) GBR bed-load carbonates (Sr ranges from 1.86 to 5.43 mmol/kg) shows that their Sr values are much higher than ours because their procedure dissolved all the carbonate in the bed-load. Our oxalate sediment procedure extracted only the exchangeable and adsorbed trace metals from the sediment samples. Because there is no calcium found in the oxalate samples, the carbonates apparently either were not dissolved by our extraction method or were only a minor component of the sediment. The exchangeable $^{87}Sr/^{86}Sr$ analyses on the sediment oxalates were not biased by carbonate dissolution, as far as we can determine. The trend toward seawater Sr values (0.0709) at Laxmipur reflects seawater flooding, not carbonate dissolution (bed-load $CaCO_3 \approx 0.72$; Galy et al., 1999). The XRD analysis did not show significant dolomite or calcite peaks, and it could be that the groundwater has dissolved most of the detrital carbonate that originally existed. Once the bed-load carbonates are deposited in the floodplain sediments and weathered by chemical dissolution, they are the major source of strontium to both the river water and the groundwater, although the radiogenic (high $^{87}Sr/^{86}Sr$) signal partially may come from silicates. The floodplain sediments not affected by seawater flooding (e.g., river samples) have high exchangeable $^{87}Sr/^{86}Sr$ ratios that influence the river and groundwater Sr isotopic chemistry through cation exchange and adsorption and desorption reactions. These phenomena explain the decreasing $^{87}Sr/^{86}Sr$ ratios from the upper section of the GBR to the lower part of the floodplain.

Shallow groundwater ($<$20 m) influences the chemistry of the GBR by discharging directly into the rivers that eventually flow into the Bay of Bengal, while the deeper groundwater discharges directly into the bay through submarine discharge. We believe that the similar groundwater and river water isotopic ratios in the GBR floodplain result from shallow groundwater discharge into the GBR, and the sediments buffer the isotopic ratios through exchange and adsorption of both the river and groundwater (Fig. 7). The strong positive correlation of Sr with HCO_3 and Ca suggests that carbonate weathering controls the input of Sr to groundwater, although the levels of Sr are reduced by subsequent adsorption to sediment (Figs. 4 and 5). In contrast to Ba, which is strongly adsorbed on river sediment ($K_d = 786 \pm 98$ mL/g), the poorly adsorbed Sr ($K_d = 7 \pm 2$ mL/g) cannot be the source of groundwater strontium. Only the rapid weathering of carbonates can provide sufficient Sr to the groundwater. If the shallow groundwater, which has on the average 7 times the dissolved Sr of the GBR water, is contributing to the GBR, why isn't the concentration of Sr in the riverine water higher? We propose that as the shallow Sr-rich and bicarbonate-rich groundwater enters the river, strontium exchanges with the riverbed sediments and suspended load and/or precipitates out with calcium carbonate. The average calculated K_d value (7 ± 2 mL/g) of the oxalate extractable Sr of the riverbed sediments shows that some Sr adsorption onto river sediments does occur.

Geochemical models as well as the budgets and residence times of elements in the ocean will need to include estimates from groundwater discharge. Oceanic residence times of trace metals are determined by dividing the total seawater concentration by the yearly mean river input. Other elements mobilized in groundwater can have a sizable submarine flux into the oceans (Table 6) and need to be included as an input in the residence time estimations.

6. CONCLUSIONS

Strontium and barium groundwater flux from the Ganges-Brahmaputra floodplain to the coastal ocean is a multistage process. Physical weathering in the Himalayas deposits sediments in the Ganges-Brahmaputra delta. As shown by this study in the Bengal Basin, the delta has a complex hydrologic regime with heterogeneous geology and large variations in sediment permeability. The sediments influence groundwater and river water chemistry through sediment permeability, cation exchange, and adsorption and desorption reactions. Carbonate dissolution, minor silicate weathering, and FeOOH breakdown contribute Ba and radiogenic Sr to the groundwater, and adsorption and desorption reactions on the fine-grained sediments control the concentrations of Sr and Ba in the groundwater. Bulk sediments with high exchangeable $^{87}Sr/^{86}Sr$ values buffer the isotopic ratios of the groundwater and river water through exchange and adsorption. The floodplain sediments not affected by seawater flooding (e.g., river samples) influence the river and groundwater Sr isotopic chemistry through cation exchange and adsorption and desorption reactions. This observation explains the decreasing $^{87}Sr/^{86}Sr$ ratios from the upper portion of the GBR to the lower floodplain. Ultimately, Sr and Ba are discharged to the ocean via river water and groundwater.

The calculated groundwater fluxes of Sr and Ba from the Ganges-Brahmaputra floodplain to the global ocean are estimated to be 3.3 and 1.2%, respectively, of the global continental flux. This strongly suggests that groundwater discharge into the coastal oceans is a significant source of trace metals such as Sr and Ba and influences the global Sr isotopic balance and its evolution through time. Submarine discharge from other

coastal floodplains with high precipitation rates and rapid accumulation of immature sediment, such as in the Irrawaddy, Yangtze, and Mekong, could make significant contributions to global oceanic budgets as well. These floodplains and others should be investigated to provide better estimates of the global submarine flux of trace metals and their isotopic compositions into the oceans. We might observe groundwater discharge by sampling coastal waters, looking for water column variations from the short-lived ($\tau < 1$ Ma) elements (e.g., Mn, Zn, As, Ba, Pb) and isotopic variations of elements with long residence times (e.g., Sr, U). Moore (1997) and Shaw et al. (1998) observed variations in Ba in the Bay of Bengal and South Atlantic Bight and concluded that significant groundwater discharge into the coastal oceans was occurring. By measuring a combination of chemical tracers such as barium and strontium isotopes in coastal oceans and the adjacent groundwater systems, we could effectively evaluate the contribution, influence, and extent of submarine groundwater discharge to the coastal oceans.

Acknowledgments—We are grateful to Pradeep K. Aggarwal of the International Atomic Energy Agency (IAEA), Vienna, Austria, for sponsoring the field excursions in the Bengal Basin, and the Atomic Energy Agency and the Water Development Board of Bangladesh (BWDB) and the Central Groundwater Board of West Bengal, India, for field support. In particular, we are appreciative of Reazuddin Ahmed and Mizanur Rahman of the BWDB and K. M. Kulkarni, now of the IAEA in Vienna, for their assistance and guidance in the field procurement of the groundwater samples in Bangladesh and West Bengal, India, respectively. We thank Billy Moore from the University of South Carolina for the GBR sediment samples and Andrew G. Hunt, Magdalyn J. Renz, Gregory L. Wortman, Scott L. Peters, and Aniki Saha for lab assistance. We also would like to express our thanks to Dr. Frank Podosek and the anonymous reviewers for their constructive comments and suggestions. This research was partially funded by National Science Foundation grant 9730743.

Associate editor: Frank Podosek

REFERENCES

Basu A. R., Poreda R. J., Smith A. A., and Aggarwal P. K. (1999) Large groundwater flux of radiogenic Sr to the Bay of Bengal and the marine Sr isotopic record. Eos: Trans. *Am. Geophys. Union* **80,** 478.

Basu A. R., Jacobsen S. B., Poreda R. J., Dowling C. B., and Aggarwal P. K. (2001) Large groundwater strontium flux to the oceans from the Bengal Basin and the marine strontium isotope record. *Science* **293,** 1470–1473.

Blum J. D., Gazis C. A., Jacobson A. D., and Chamberlain C. P. (1998) Carbonate versus silicate weathering in the Raikot watershed within the High Himalayan Crystalline Series. *Geology* **26**(5), 411–414.

Bokuniewicz H. and Pavlik B. (1990) Groundwater seepage along a barrier island. *Biogeochemistry* **10,** 257–276.

British Geological Survey (1999) Main report. In *Groundwater Studies for Arsenic Contamination in Bangladesh*. Department of International Development.

Burnett W. C., Cowart J. B., and Deetae S. (1990) Radium in the Suwannee River and estuary. *Biogeochemistry* **10,** 237–255.

Carey A. E. and Wheatcraft S. W. (1995) Parametric study of salt water intrusion. *Geol. Soc. Am. Abst. Progr.* **27,** 260.

Carey A. E., Wheatcraft S. W., Glass R. J., and O'Rourke J. P. (1995) Non-Fickian ionic diffusion across high-concentration gradients. *Water Resources Res.* **31**(9), 2213–2218.

Cerling T. E. and Spalding B. P. (1982) Distribution and relationship of radionuclides to streambed gravels in a small watershed. *Environ. Geol.* **4,** 99–116.

Cerling T. E. and Turner R. R. (1982) Formation of freshwater Fe-Mn coatings on gravel and the behavior of ^{60}Co, ^{90}Sr, and ^{137}Cs in a small watershed. *Geochim. Cosmochim. Acta* **46,** 1333–1343.

Chaudhuri S. and Clauer N. (1986) Fluctuations of isotopic composition of strontium in seawater during the Phanerozoic Eon. *Chem. Geol.* **59,** 293–303.

Chesley J. T., Quade J., and Ruiz J. (2000) The Os and Sr isotopic record of Himalayan paleorivers: Himalayan tectonics and influence of ocean chemistry. *Earth Planet. Sci. Lett.* **179,** 115–124.

Clarke W. B., Jenkins W. J., and Top Z. (1976) Determination of tritium by mass spectrometric measurement of ^{3}He. *Int. J. Appl. Radiat. Isot.* **27,** 515–522.

Coleman J. M. (1969) Brahmaputra River: Channel processes and sedimentation. *Sediment. Geol.* **3**(2/3), 129–239.

Cummings D. E. Jr., Caccavo F., Fendorf S., and Rosenzweig RF. (1999) Arsenic mobilization by the dissimilatory Fe(III)-reducing bacterium Shewanella alga BrY. *Environ. Sci. Technol.* **33,** 723–729.

Derry L. A. and France-Lanord C. (1996) Neogene Himalayan weathering history and river ^{87}Sr/^{86}Sr: Impact on the marine Sr record. *Earth Planet. Sci. Lett.* **142,** 59–74.

Dowling C. B., Poreda R. J., Peters S. L., Basu A. R., and Aggarwal P. K. (1999) Groundwater flux of trace elements in the Ganges-Brahmaputra flood plain Eos: Trans. *Am. Geophys. Union* **80,** 431.

Dowling C. B., Poreda R. J., Basu A. R., Aggarwal P. K. (in press) A geochemical study of arsenic release mechanisms in the Bengal Basin groundwater. Water Resources Res 38(9):1173–1190.

Edmond J. M. (1992) Himalayan tectonics, weathering processes, and the strontium isotope record in marine limestones. *Science* **258,** 1594–1597.

English N. B., Quade J., DeCelles P. G., and Garzione C. N. (2000) Geologic control of Sr and major element chemistry in Himalayan Rivers, Nepal. *Geochim. Cosmochim. Acta* **64,** 2549–2566.

Fehn U., Synder G., and Egeberg P. K. (2000) Dating of pore waters with ^{129}I; relevance for the origin of marine gas hydrates. *Science* **289,** 2332–2335.

Fetter C. W. (1988) *Applied Hydrogeology*. Merrill, Columbus, OH.

Food and Agriculture Organization. (1971) *Soil Survey Project, Bangladesh*. United Nations Development Programme, Food and Agriculture Organization.

Galy A. and France-Lanord C. (1999) Weathering processes in the Ganges-Brahmaputra basin and the riverine alkalinity budget. *Chem. Geol.* **159,** 31–60.

Galy A. and France-Lanord C. (2001) Higher erosion rates in the Himalaya: Geochemical constraints on riverine fluxes. *Geology* **29**(1), 23–26.

Galy A., France-Lanord C., and Derry L. (1999) The strontium isotopic budget of Himalayan Rivers in Nepal and Bangladesh. *Geochim. Cosmochim. Acta* **63,** 1905–1925.

Giblin A. E. and Gaines A. G. (1990) Nitrogen inputs to a marine embayment: The importance of groundwater. *Biogeochemistry* **10,** 309–328.

Godderis Y. and Francois L. M. (1995) The Cenozoic evolution of the strontium and carbon cycles: Relative importance of continental erosion and mantle exchanges. *Chem. Geol.* **126,** 169–190.

Greenberg A. E., Clesceri L. S., and Eaton A. D. (1992) *Standard Methods for the Examination of Water and Wastewater*. American Public Health Association, Washington, DC.

Harris N. (1995) Significance of weathering Himalayan metasedimentary rocks and leucogranites for the Sr isotope evolution of seawater during the early Miocene. *Geology* **23**(9), 795–198.

Holeman J. N. (1968) The sediment yield of major rivers in the world. *Water Resources Res.* **4**(4), 737–747.

Hunt A. G. (2000) *Diffusional Release of Helium-4 From Mineral Phases as Indicators of Groundwater Age and Depositional History*. Ph.D. dissertation, University of Rochester.

Hunt A. G., Poreda R. J., and Solomon D. K. (2000) Factors controlling the release of ^{3}He, ^{4}He, and ^{21}Ne in quartz. Eos Transactions 81(48):F447–448.

Johannes R. E. (1980) The ecological significance of the submarine discharge of groundwater. *Mar. Ecol. Prog. Ser.* **3,** 365–373.

Johnston H. M. and Gillham R. W. (1984) Natural Sr concentrations and K_d determinations. *J. Geotech. Eng.* **110**(10), 1459–1472.

Johnston H. M., Gillham R. W., and Cherry J. A. (1985) Distribution coefficients for strontium and cesium in overburden at a storage area for low-level radioactive waste. *J. Can. Geotech.* **22,** 6–16.

Kaufman S. and Libby W. F. (1954) The natural distribution of tritium. *Phys. Rev.* **93,** 1337–1344.

Krishnaswami S., Trivedi J. R., Sarin M. M., Ramesh R., and Sharma K. K. (1992) Strontium isotopes and rubidium in the Ganga-Brahmaputra river system: Weathering in the Himalaya, fluxes to the Bay of Bengal and contributions to the evolution of oceanic $^{87}Sr/^{86}Sr$. *Earth Planet. Sci. Lett.* **109,** 243–253.

LaPointe B. E., O'Connell J. D., and Garrett G. S. (1990) Nutrient couplings between on-site sewage disposal systems, groundwaters, and nearshore surface waters of the Florida Keys. *Biogeochemistry* **10**(3), 289–307.

Liszewski M. M., Rosentreter J. J., Miller K. E., and Bartholomay R. C. (2000) Chemical and physical properties affecting strontium distribution coefficients at surficial-sediment samples at the Idaho National Engineering and Environmental Laboratory, Idaho. *Environ. Geol.* **39**(3/4), 411–426.

Loeb S. L. and Goldman C. R. (1979) Water and nutrient transport via groundwater from Ward Valley into Lake Tahoe. *Limnol. Oceanogr.* **24**(6), 1146–1154.

Long S. E. and Martin T. D. (1991) Method 2008: Determination of trace elements in waters and wastes by inductively coupled plasma-mass spectrometry. In *Methods for the Determination of Metals in Environmental Samples* (ed. U. S. Environmental Protection Agency), pp. 83–122. U.S. Environmental Protection Agency, Washington, DC.

McArthur J. M., Ravenscroft P., Safiullah S., and Thirlwall M. F. (2001) Arsenic in groundwater: Testing pollution mechanisms for sedimentary aquifers in Bangladesh. *Water Resources Res.* **37**(1), 109–117.

McKeague J. A. (1978) *Manual on Soil Sampling and Methods of Analysis*. Canadian Society of Soil Science, Pinawa, Canada.

Milliman J. D. and Meade R. H. (1983) World-wide delivery of river sediment to the oceans. *J. Geol.* **91**(1), 1–21.

Moore W. S. (1996) Large groundwater inputs to coastal waters revealed by ^{226}Ra enrichments. *Nature* **380,** 612–614.

Moore W. S. (1997) High fluxes of radium and barium from the mouth of the Ganges-Brahmaputra river during low river discharge suggest a large groundwater source. *Earth Planet. Sci. Lett.* **150,** 141–150.

Morgan J. P. and McIntire W. G. (1959) Quaternary geology of the Bengal Basin, East Pakistan and India. *Bull. Geol. Soc. Am.* **70,** 319–342.

Oberdorfer J. A., Valentino M. A., and Smith S. V. (1990) Groundwater contribution to the nitrogen budget of Tomales Bay, California. *Biogeochemistry* **10,** 199–216.

Palmer M. R. and Edmond J. M. (1989) The strontium isotope budget of the modern ocean. *Earth Planet. Sci. Lett.* **92,** 11–26.

Palmer M. R. and Edmond J. M. (1992) Controls over the strontium isotope composition of river water. *Geochim. Cosmochim. Acta* **56,** 2099–2111.

Poreda R. J. and Farley K. A. (1992) Rare gases in Samoan xenoliths. *Earth Planet. Sci. Lett.* **113,** 129–144.

Poreda R. J., Cerling T. E., and Solomon D. K. (1988) Tritium and helium isotopes as hydrologic tracers in a shallow unconfined aquifer. *J. Hydrol.* **103**(1–2), 1–9.

Quade J., Roe L., DeCelles P. G., and Ojha T. P. (1997) The late Neogene $^{87}Sr/^{86}Sr$ record of the lowland Himalayan rivers. *Science* **276,** 1828–1831.

Raymo M. E., Ruddiman W. F., and Froelich P. N. (1988) Influence of late Cenozoic mountain building on ocean geochemical cycles. *Geology* **16,** 649–153.

Richter F. M., Rowley D. B., and DePaolo D. J. (1992) Sr isotope evolution of seawater: The role of tectonics. *Earth Planet. Sci. Lett.* **109,** 11–23.

Robertson W. D. and Cherry J. A. (1989) Tritium as an indicator of recharge and dispersion in the groundwater system in Central Ontario. *Water Resources Res.* **25**(6), 1097–1109.

Sarin M. M., Krishnaswami S., Dilli K., Somayajulu B. L. K., and Moore W. S. (1989) Major ion chemistry of the Ganges-Brahmaputra river system: Weathering processes and fluxes to the Bay of Bengal. *Geochim. Cosmochim. Acta* **53,** 997–1009.

Schlosser P. (1992) Tritium/^{3}He dating of waters in natural systems. In *Isotopes of Noble Gases as Tracers in Environmental Studies* (eds. H. H. Loosli and E. Mazor), pp. 123–145. International Atomic Energy Agency, Vienna, Austria.

Shaw T. J., Moore W. S., Kloepfer J., and Sochaski M. A. (1998) The flux of barium to the coastal waters of the southeastern USA: The importance of submarine groundwater discharge. *Geochim. Cosmochim. Acta* **62,** 3047–3054.

Singh S. K., Trivedi J. R., Pande K., Ramesh R., and Krishnaswami S. (1998) Chemical and strontium, oxygen, and carbon isotopic compositions of carbonates from the Lesser Himalaya: Implications to the strontium isotope composition of the source waters of the Ganga, Ghaghara, and the Indus rivers. *Geochim. Cosmochim. Acta* **62,** 743–755.

Solomon D. K., Poreda R. J., Schiff S. L., and Cherry J. A. (1992) Tritium and helium-3 as groundwater age tracers in the Borden Aquifer. *Water Resources Res.* **28**(3), 741–755.

Solomon D. K., Schiff S. L., Poreda R. J., and Clarke W. B. (1993) A validation of the $^3H/^3He$ method for determining groundwater recharge. *Water Resources Res.* **29,** 2951–2962.

Solomon D. K., Poreda R. J., Cook P. G., and Hunt A. (1995) Site characterization using $^3H/^3He$ ground-water ages, Cape Cod, MA. *Ground Water* **33**(6), 988–996.

Solomon D. K., Hunt A., and Poreda R. J. (1996) Source of radiogenic helium-4 in shallow aquifers: Implications for dating young groundwater. *Water Resources Res.* **32**(6), 1805–1813.

Stallard R. F. and Edmond J. M. (1983) Geochemistry of the Amazon 2. The influence of geology and the weathering environment on the dissolved load. *J. Geophys. Res.* **88**(C14), 9671–9688.

Stallard R. F. and Edmond J. M. (1987) Geochemistry of the Amazon 3. Weathering chemistry and limits to dissolved inputs. *J. Geophys. Res.* **92**(C8), 8293–8302.

Subramanian V. (1979) Chemical and suspended sediment characteristics of rivers of India. *J. Hydrol.* **44,** 37–55.

To T. B., Nordstrom D. K., Cunningham K. M., Ball J. W., and McCleskey R. B. (1999) New method for the direct determination of dissolved Fe(III) concentration in acid mine waters. *Environ. Sci. Technol.* **33,** 807–813.

Uddin A. and Lundberg N. (1998) Cenozoic history of the Himalayan-Bengal system: Sand composition in the Bengal Basin, Bangladesh. *Geol. Soc. Am. Bull.* **110,** 497–511.

Valiela I., Costa J., Foreman K., Teal J. M., Howes B., and Aubrey D. (1990) Transport of groundwater-borne nutrients from watersheds and their effects on coastal waters. *Biogeochemistry* **10,** 177–197.

Valiela I., Foreman K., LaMontagne M., Hersh D., Costa J., Peckol P., DeMeo-Anderson B., D'Avanzo C., Babione M., Sham C-H., Brawley J., and Lajtha K. (1992) Couplings of watersheds and coastal waters: Sources and consequences of nutrient enrichment in Waquoit Bay, Massachusetts. *Estuaries* **15**(4), 443–457.

Wheatcraft S. W. and Burns E. R. (1997) A sandbox model of seawater intrusion: Validation of density-coupled flow and transport models. *Geol. Soc. Am. Abst. Progr.* **29,** 73.